Sensitivity to Nuclear Data and Neutron Source Type in Calculations of Transmutation Capabilities of the Energy Amplifier Demonstration Facility

M. Dahlfors

Department of Radiation Sciences
Uppsala University

Licentiate Thesis

May 2003

Abstract

This text, which is a thesis for the degree "filosofie licentiat", is a summary of two studies the author has performed within the field of 3-D Monte Carlo calculations of Accelerator Driven Systems (ADS) for transmutation of nuclear waste. The simulations were carried out with the state-of-the-art computer code package EA-MC, developed by C. Rubbia and his group at CERN. The concept studied is ANSALDOs 80 MW_{th} Energy Amplifier Demonstration Facility based on classical MOX-fuel technology and on molten Lead-Bismuth Eutectic cooling. A review of neutron cross section sensitivity in numerical calculations of an ADS and a comparative assessment relevant to the transmutation efficiency of plutonium and minor actinides in fusion/fission hybrids and ADS are presented.

Contents

List of Papers

1. Dahlfors, M., Kadi, Y., *Sensitivity Analysis of Neutron Cross Sections Relevant for Accelerator Driven Systems.* Journal of Nuclear Science and Technology, Supplement 2, p. 1198-1201, August 2002. Also published in a more comprehensive form in C. Rubbia, M. Dahlfors, Y. Kadi, *Sensitivity Analysis of Neutron Cross Sections Relevant for Accelerator Driven Systems*, in 1st Management Report of the nTOFND-ADS EC programme under contract no. FIKW-CT-2000-00107.

2. M. Dahlfors, Y. Kadi, *Comparative Assessment of the Transmutation Efficiency of Plutonium and Minor Actinides in Fusion/Fission Hybrids and ADS*, Proceedings of 6th Information Exchange Meeting on Actinide and Fission Product Partitioning and Transmutation, 11-13 December 2000, Madrid, Spain. CERN EET Internal Note 2000-012.

1 Introduction

The International Energy Agency (IEA) predicts that the world's energy consumption will increase by two thirds until 2030 and that electricity use will grow faster than any other energy end-use [1], see Figure 1.1. It is thus urgent to make plans for how this demand should be met with as sustainable energy forms as possible.

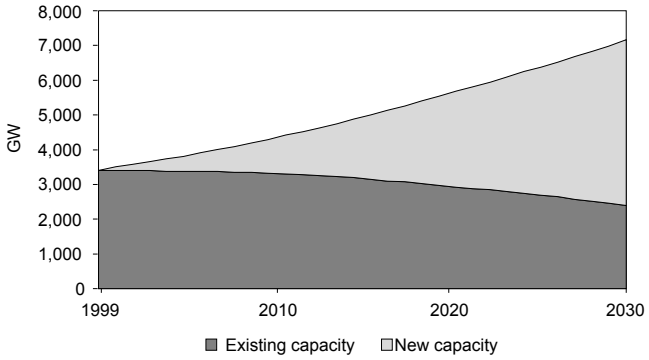

Figure 1.1 World installed electricity generation capacity and expected increase until 2030.

The classic energy forms that dominate the market and currently are utilised for large-scale energy production are quite readily extracted and thus come at a reasonable cost; fossil fuel-based (coal, oil and gas), hydroelectric and nuclear energy. The timescale for the cost of each is different, the initial investment being larger for hydroelectric and nuclear, whereas the fuel cost itself dominates the cost for fossil fuel-based energy. On the long term, hydroelectric power is a winner due to low maintenance and non-existent fuel expenses.

There are evident limitations in the availability of the fuel resources. The cheapest energy production form, hydroelectric, is in many areas a stable electricity supplier, as long as precipitation stays stable from year to year. However, there are only a finite amount of rivers that can be exploited, so in this respect there is a limit for how much hydroelectric power can be produced, even if the "fuel resource" itself is inexhaustible. The availability limitations particularly apply to the case of fossil fuels. Worldwide recoverable coal reserves are estimated

to last for another 200 years at current rates of exploitation [2]. Concerning natural gas and oil, the values given are 60 and 40 years, respectively. It should be noted that these values are not accurate estimates, but only a simple division of the amount of reserves with the current production rate, i.e. no attention is paid to future growth in demand. Ultimately, as production declines and cost goes up, there will have to be a replacement for oil as the most important energy source.

Similar arguments as above can be applied to the availability of uranium for nuclear energy production, but there are several reservations that need to be made. Firstly, uranium is abundant on many locations, forming about two parts per million of the Earth's crust, which makes it 500 times more abundant than gold, 40 times as common as silver and slightly more abundant than tin. At a roughly estimated (and optimistic) average rate of consumption at 75,000 tU/year for the period between 2002 and 2041 it could be assessed that this low-price supply would only suffice until the end of the same period [3]. Still undiscovered resources have the potential of extending this period with a factor of three. However, it needs to be pointed out that the uranium price does not significantly affect the production costs for nuclear power, and thus even lower grade uranium ore at a higher cost can be utilised without any larger economic consequences. Secondly, the fissile isotope ^{235}U is only present to 0.7% in the natural uranium (U_{nat}), the rest mostly consisting of the fertile ^{238}U, and the uranium must be enriched up to 3-5% in ^{235}U for use in conventional light water reactors (LWR)[1]. In practical terms, this means that about six units of U_{nat} is needed for one unit of reactor grade uranium. However, if fertile isotopes were to be utilised in the power production, the potential nuclear fuel resources become vast indeed. Significant research and development efforts have been and are put on systems that use fast neutrons, which has produced a flora of promising new concepts for fast reactors (FR) and accelerator driven systems (ADS), see Section 3. It has been estimated that nuclear fuel resources could be extended by a factor 100 if a strategy including these systems were to be implemented [4]. Thirdly and lastly, there is an important alternative fuel, thorium, that could be employed for nuclear energy production. Thorium is three times more abundant than uranium in the earth's rocks and soil, with economically recoverable world thorium reserves even surpassing the uranium reserves.

When environmental issues and social acceptance are taken into consideration, the issue of future energy sources becomes more complex. Large-scale hydroelectric plants have an impact on local ecosystems and in some cases also on human habitation. Even smaller-scale plants affect local lake, river and/or naval ecosystems; particularly local fishery may suffer. Public concern for carbon

[1] The term "fissile" refers to isotopes which undergo fission by thermal neutrons, whereas "fertile" implies those isotopes that are not fissioned by thermal neutrons, but which can undergo fission with fast neutrons and/or be transmuted into fissile isotopes by neutron capture. The latter process is often referred to as "breeding".

dioxide releases and a possibly ensuing global warming has already incited world leaders to sign international agreements on carbon dioxide releases and decrease thereof, most importantly the Kyoto Protocol that stipulates the greenhouse gas emission limitations or reduction commitments of the signing countries. The climate policy adopted in the Kyoto Protocol is now a fact; it is clear that developed countries will not be able to unconditionally extend their energy use in the future with fossil fuel-based energy.

The already existing option is naturally nuclear power, which can be considered to offer the only truly long-term solution for large-scale energy production. Nuclear power in its turn has suffered from public distrust since the 1970's, largely due to the reactor incidents at Three Mile Island in 1979 and at Chernobyl in 1986. The effect of the negative public opinion has perhaps in the end proved, if not useful, but essential to the nuclear industry, which now shows more openness towards the public than the industry in general. Furthermore, extremely high safety standards have been implemented, and thus the nuclear power industry has grown more mature to take on a larger responsibility for the world's energy production. If it is proven that nuclear reactors can be operated at absolutely safe conditions, e.g. by proven passive safety measures and multiple protection measures, then only one major obstacle remains from gaining thorough public acceptance, namely the waste issue. It seems difficult to gain firm public support for the geological disposal alternative: little interest is often shown by the local populations of the candidate sites and the idea that nuclear waste could be contained for millions of years without radiotoxic elements leaking to the biosphere is questionable. The proliferation issue is also of some importance; how can these storages be protected from future intentional or even unintentional intrusion?

The problem has lately been addressed by the development of accelerator driven systems (ADS) for transmutation of nuclear waste, which are dedicated nuclear waste incineration systems having the potential to efficiently reduce waste volumes and shorten storage times from millions of years to hundreds of years. ADS addresses the safety aspects of burning nuclear waste[2] since the system is source-driven and therefore can be operated in a subcritical mode with larger reactivity margins. Many of the suggested ADS concepts also employ passive safety systems concerning coolant flow and accelerator beam shutoff. In order for nuclear energy to provide an important contribution to the sustainable energy development of the future, successful implementation of ADS technology for nuclear waste treatment may prove essential.

[2]When using minor actinides as fuel, the reactivity margins are smaller. This is a cause for concern in critical systems.

2 Nuclear Waste

The primary purpose of accelerator driven systems is to destroy the most radiotoxic and long-lived components of nuclear waste. Nuclear waste can primarily be classified as high-level (HLW) and low-level waste (LLW). HLW consists of highly radioactive fission and capture products arising in the nuclear fuel, whereas LLW represents waste produced during operation of nuclear facilities, e.g. activated machine parts, structural materials, protectional clothing and residues from medical and industrial use of radionuclides. The concept of accelerator driven transmutation of nuclear waste applies to HLW.

The constituents of HLW in their turn are often classified in two groups: transuranic elements[1] and fission products. Transuranic elements (TRU) are activation products arising from uranium isotopes and yield the most significant contribution of long-lived radiotoxicity to nuclear waste. Representative for the TRU category are the Pu isotopes and the minor actinides (MA) Np, Am and Cm. Table 2.1 gives an overview of the TRU masses in LWR spent fuel after 15 years of cooling time.

Table 2.1 Transuranics in LWR spent fuel (40 GWd/ton U) after 15 years decay, from [5].

Nuclide	Amount [g/ton]	Nuclide	Amount [g/ton]
Np-236	5.30E-04	Am-242m	2.50E+00
Np-237	6.50E+02	Am-243	1.40E+02
Pu-238	2.30E+02	Cm-242	5.90E-03
Pu-239	5.90E+03	Cm-243	4.30E-01
Pu-240	2.60E+03	Cm-244	3.10E+01
Pu-241	6.80E+02	Cm-245	2.30E+00
Pu-242	6.00E+02	Cm-246	3.20E-01
Pu-244	4.20E-02	Cm-247	3.70E-03
Am-241	7.70E+02	Cm-248	2.40E-04

[1]Some of the TRUs are sometimes regarded as forming their own group of nuclear waste alongside HLW and LLW, due to the fact that they are not radioactive enough to strictly qualify as HLW.

Radionuclides produced by nuclear fission are referred to as fission products. The majority of these are reasonably short-lived and decay into stable nuclides within human timescales, and are thus fairly unproblematic from a radiotoxicity point of view. However, some of the fission products are produced in significant quantities and decay slowly. These are known as the long-lived fission products (LLFP). Out of the LLFP, two major contributors to the long-term risk of HLW repositories can be transmuted, namely ^{129}I and ^{99}Tc. It should be noted that ^{129}I and ^{99}Tc represent 95% of the LLFF class A storage volume [6].

The HLW is contained in the spent fuel, which on the other hand is composed to $> 90\%$ of ^{238}U. It would be of interest to separate the depleted uranium from the HLW, since its share of the volume is great and it contributes only modestly to the potential radiotoxicity, i.e. it would not need to be stored as rigorously as the HLW, at the same time as it is fertile and a possible fuel material for the future. This fact has lead to some countries choosing a *fuel reprocessing* strategy for their nuclear waste treatment, i.e. the uranium and plutonium is recovered from the fuel while the remaining HLW (consisting mostly of fission products and MA) is isolated in liquid and solid fuel reprocessing products. Fuel reprocessing reduces the potential long-term radiotoxicity by a factor of 10 due to removal of plutonium and the waste volume to an even larger extent due to removal of uranium [7]. However, it then follows that the plutonium must be burnt, otherwise the procedure would only separate one type of waste from another. Currently, the world's plutonium stockpile is only growing, primarily due to worldwide reductions of nuclear weapons arsenals. Hence, the demand for waste incineration – and in particular plutonium burning – techniques is also increasing.

3 Accelerator Driven Systems

The concept of transmutation dates back as early as 1919, when Rutherford first transmuted ^{14}N to ^{17}O using energetic α-particles. Following the development of high power accelerators in the 1940's, the first large-scale proposal for producing neutrons by spallation with an accelerator was made by Lawrence in 1950. The project was code-named Material Testing Accelerator (MTA), but the aim was to produce plutonium from depleted uranium. The MTA project was abandoned after four years, and spallation-driven transmutation received little attention until the late 1980's, when interest was renewed particularly in the U.S. and Japan, then with rather the opposite objective – to destroy nuclear waste, i.e. plutonium and minor actinides. Since then, a number of research groups around the world have worked intensely within the field of accelerator driven systems (ADS), accelerator driven transmutation of waste (ATW) and hybrid systems, which are all different flavours of systems based on an accelerator driven spallation source coupled with a subcritical core.

In the exploratory phase of ADS development, both thermal and fast neutron systems were suggested. However, as simulation tools improved and the goal was clarified to be waste incineration (rather than energy production), systems using *fast neutrons* have been established as standard, since only modest radiotoxicity reductions can be reached with a thermal system. Another specialty is the core of an ADS, which is *subcritical* and must be driven by externally produced neutrons. As the name indicates, an ADS makes use of an accelerator for delivering protons (kinetic energy of typically 1 GeV), which in turn produce source neutrons via nuclear intranuclear cascade processes in a spallation target, thus providing the external neutron source. The basic concept scheme for an ADS is depicted in Figure 3.1. The subcriticality feature is a central issue, since it allows for larger reactivity margins during operation, independently of the delayed neutron fractions, β, of the fuel material. MA and plutonium both in general share the property of having markedly smaller β values than uranium; reactor safety considerations would seriously limit the loading of MA in a critical fast reactor (FR) core. Due to this fact and the FR's generally positive reactivity coefficients without ^{238}U, it is virtually impossible to burn MA in the FR unless adding a significant quantity of ^{238}U. Such a measure should be avoided, however, since it would mean further buildup of MA and breeding of more plutonium from ^{238}U. With an ADS, on the other hand, such problems can be avoided, since its sub-

criticality will be the important safety parameter that determines the reactivity margin.

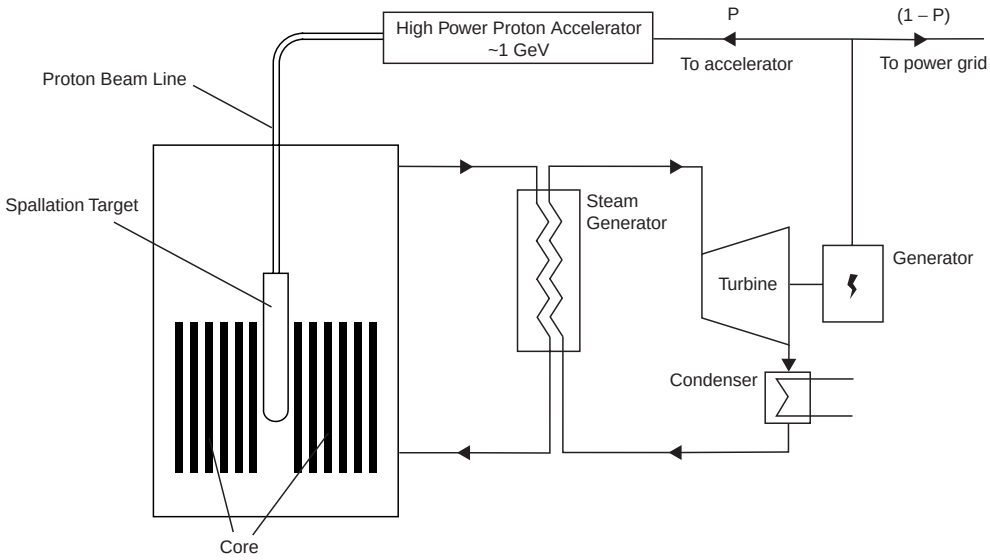

Figure 3.1 Basic concept of an accelerator driven system

As is seen from Figure 3.1, the ADS power production scheme is fairly similar to the one of conventional electricity generation. The heat produced in the fuel is transported with the coolant to heat exchangers, where steam is produced to drive a turbine and consequently an electricity generator. The difference is that part of the electricity must be fed to the proton accelerator to keep the external neutron source running. The core structure itself is also fairly similar to classic ones; most ADS concepts envisage the fuel loaded according to well-known and proven technology, in fuel rods. The fuel composition, as mentioned above, naturally distinguishes the system from conventional nuclear reactors. Another vital difference is the coolant material, which must be sufficiently "transparent" to neutrons. The neutrons need to retain a large part of their energy after each collision, since the system is desired to work with fast neutrons. The most commonly suggested coolant material is a lead-bismuth eutectic mixture, but also sodium-cooled and gas-cooled systems have been proposed.

Numerical calculations of ADS system parameters and simulation of the system behaviour requires special tools. A conventional nuclear reactor simulation code is not directly applicable for a number of reasons [8], of which perhaps the most important is the spatial distribution of the neutron flux decreasing in an exponential manner in the radial direction out from the spallation source in the center of the core. In a critical reactor, the flux distribution is instead essentially

of a cosine form and determined by the geometrical constraints of the setup [9]. The neutron source, its geometrical form and the associated spallation processes have to be simulated correctly in order to determine the flux distributions. Monte Carlo techniques have been established as the most suitable simulation method for the purpose of exploratory and yet accurate calculations of ADS, but there are only a few codes that are suited particularly for ADS. The most specialised computer code package for the application, EA-MC, was developed by C. Rubbia and his group at CERN and is to date the only simulation package integrating neutron transport and evolution of the material composition in the same code [10]. Other important codes suitable for ADS simulation are represented by MCNP-4, MCNP-X and the deterministic alternative ERANOS.

The calculations and results of this thesis are based on the particular ADS reference configuration known as the Energy Amplifier Demonstration Facility (EADF) [11]. The system was developed with the Energy Amplifier (EA) as the conceptual basis [12]. The EADF is described in detail in the papers and the references. All simulations were performed with EA-MC.

4 Overview of the Papers

The fundamental technologies needed for realisation of ADS are essentially known, but before a full-scale, operative waste-burning and power-producing ADS can be built, refinement of the knowledge about how such a system behaves in reality is needed. At the same time, simulation tools also have to be developed so as to accurately predict the behaviour of an ADS.

Except for the physical models, the accuracy of the predictions that a computer code makes is dependent of the data it uses. In the case of numerical simulation of ADS, the vital input is provided by the nuclear data libraries. The IAEA ADS Neutronic Benchmark (Stage 1) [13] showed that there are significant weaknesses particularly concerning the neutron cross sections relevant to ADS calculations. The shortcomings from the ADS point of view are the fact that neutron cross section data are not given for higher energies than 20 MeV, that large discrepancies are found even by direct comparison of cross sections between the different libraries and in some cases, that data are non-existent for certain isotopes. The lack of reliable data has incited several neutron cross section measurement experiments like the nTOF experiment [14] presently being conducted at CERN. It is beneficial for the outcome of these experiments to assess how priorities should be set from the ADS standpoint for the nuclides to be measured, i.e. which isotopes and reaction channels are of extraordinary importance for ADS simulation purposes. This was the point of departure for the work described in Paper 1, *Sensitivity Analysis of Neutron Cross Sections Relevant for Accelerator Driven Systems*. The results indicate that the discrepancies between cross sections given by different nuclear data libraries are large enough to account for a subsequent difference in the multiplication factor almost of the order of its subcriticality margin, a clear sign that the data are inadequate for ADS simulation purposes. Here, it should be noted that the difference between the libraries in no way describes the actual uncertainty, which may be larger. Indications are also given on which isotopes deserve more attention, and in this context perhaps the remarkable differences found for the cross sections of the lead isotopes should be pointed out, since they account for such a large quantity of material in the core of the EADF.

Three zero-power subcritical core experiments, which also address the issues mentioned in the beginning of this section, have been or are being performed: the First Energy Amplifier Test (FEAT) at CERN in 1994 [15, 16], the still on-going

Yalina Experiment or ISTC-B70 in Minsk, Belarus [17] and the also on-going MUSE (MUltiplication de Source Externe) Experiment at CEA Cadarache [18]. The main purpose of these experiments is to gain information on the physics of subcritical systems and to provide data for computer code validation; both Yalina and MUSE are benchmark exercises supported by the IAEA. Yalina and MUSE have in common that they employ only fission and fusion neutron sources, mainly due to practical considerations: building a high-power accelerator where it does not already exist is costly. This formed the incentive for Paper 2, *Transmutation Efficiency of Plutonium and Minor Actinides in Fusion/Fission Hybrids and ADS*, where the transmutation efficiency of the EADF is examined and compared for different neutron source types. The results indicate that the fusion-DD source would better emulate the multiplication factor and the neutron balance obtained with a spallation source, while other properties of the system may be as well (or even slightly better) simulated with the fusion-DT source. The effect on transmutation efficiency seems reasonably unaffected by the choice of source. For reasons of complementarity, application of both source types in coming experiments appears reasonable.

5 Prospects

The work presented in this thesis is still on-going, even if certain aspects are at a closure. The neutron cross section sensitivity study will continue with the aim of developing a more quantitative methodology. This is envisaged in either of two different ways: one is to follow the guidelines given in Paper 1, i.e. to employ deterministic methods and perform a full analysis with a cross section sensitivity-uncertainty code utilising cross section data covariance files. Another (and possibly more tedious) alternative would be the direct manipulation of neutron cross section data, either allowing it through the computer code EA-MC or doing it externally.

As such, the study of the transmutation efficiency in the EADF with different neutron sources is closed. On the other hand, the work with the Yalina experiment, which employs fusion-DD and fusion-DT neutron sources, continues and the results will be published before the end of 2003. In the context of subcritical core experiments, also a parallel code benchmarking project with the FEAT experiment as a basis will be completed.

Bibliography

[1] International Energy Agency (IEA). *World Energy Outlook 2002*. IEA Publications, 9 rue de la Fédération, 75739 PARIS CEDEX 15, France, 2002.

[2] *BP Statistical Review of World Energy 2002*, BP Distribution Services 23 Hinton Road Bournemouth, Dorset BH1 2EF, UK, 18th June 2002. Also found on http://www.bp.com/centres/energy2002/.

[3] OECD Nuclear Energy Agency and International Atomic Energy Agency. *Uranium 2001 – Resources, Production and Demand*. OECD/NEA and IAEA, 2002.

[4] OECD Nuclear Energy Agency. *Trends in the Nuclear Fuel Cycle – Economic, Environmental and Social Aspects*. OECD/NEA, 2001.

[5] The European Technical Working Group on ADS. *A European Roadmap for Developing Accelerator Driven Systems (ADS) for Nuclear Waste Incineration*, volume 3 of *Fundamental University Physics*. ENEA, Ente per le Nuove tecnologie, lEnergia e lAmbiente Lungotevere Thaon di Revel, 76 00196 Roma, 2001.

[6] C. Rubbia, S. Buono, Y. Kadi, and J.A. Rubio. *Fast Neutron Incineration in the Energy Amplifier as Alternative to Geological Storage: the Case of Spain*. Emerging Energy Technologies, SL Division, CERN, September 1995. CERN report CERN/LHC/97-01 (EET).

[7] Weston M. Stacey. *Nuclear Reactor Physics*, pages 224–239. John Wiley & Sons, 2001.

[8] Y. Kadi and F. Carminati. Simulation of accelerator-driven systems. 2001. Lecture given at the Workshop on Hybrid Nuclear Systems for Energy Production, Utilisation of Actinides & Transmutation of Long-Lived Radioactive Waste, Trieste, 3-7 September 2001.

[9] Weston M. Stacey. *Nuclear Reactor Physics*, chapter 3. John Wiley & Sons, 2001.

[10] Y. Kadi. *Neutronic Analysis of the Energy Amplifier Demonstration Facility using the EA Monte Carlo Code Package*. Emerging Energy Technologies,

SL Division, CERN, 2000. EET Internal Note 2000-009, also in *Proceedings of 4^{th} Intl. Conf. on Supercomputing in Nuclear Applications (SNA2000)*.

[11] Ansaldo Nucleare. *Energy Amplifier Demonstration Facility Reference configuration: Summary Report*. ANSALDO Nucleare, January 1999. EA-B0.00-1-200 - Rev. 0.

[12] C. Rubbia et al. *Conceptual Design of a Fast Neutron Operated High Power Energy Amplifier*. Emerging Energy Technologies, SL Division, CERN, September 1995. CERN report CERN/AT/95-44 (EET).

[13] Y. Kadi and F. Carminati. *ADS Neutronic Benchmark (stage 1)*. Emerging Energy Technologies, SL Division, CERN. EET Internal Note 98-005. Presented at IAEA Technical Committee Meeting on Feasibility and Motivation for Hybrid Concepts for Nuclear Energy Generation and Transmutation, CIEMAT, Madrid, Spain, 17-19 September 1994.

[14] *Proposal for a Neutron Time of Flight Facility*. CERN, Geneva, Switzerland, 1999. CERN/SPSC 99-8.

[15] S. Andriamonje et al. *Physics Letters B*, 348:697–709, 1995.

[16] J. Calero et al. *Nuclear Instruments and Methods A*, 376:89–103, 1996.

[17] S. Chigrinov and I. Rakhno. IAEA Benchmark 3.2: Experimental Research of Neutronics of A Subcritical Uranium-Polyethylene Assembly Driven with a Neutron Generator (The Yalina Experiment). Technical report, Radiation Physics and Chemistry Problems Institute, National Academy of Sciences, Republic of Belarus, Minsk, 2000.

[18] M. Salvatores et al. MUSE-1: A first experiment at MASURCA to validate the physics of sub-critical multiplying systems relevant to ADS. In *Proceedings of the 2^{nd} Intl. Conf. on ADTT*, Kalmar, Sweden, June 1996.

Sensitivity Analysis of Neutron Cross Sections Relevant for Accelerator Driven Systems

Carlo RUBBIA[1], Marcus DAHLFORS[2,3], Yacine KADI[3]

Abstract

A preliminary review of cross section sensitivity in 3-D Monte Carlo calculations of Accelerator Driven Systems has been performed. The concept studied was ANSALDO's 80 MW_{th} Energy Amplifier Demonstration Facility based on classical MOX-fuel technology and on molten Lead-Bismuth Eutectic cooling. The simulations were carried out with the state-of-the-art computer code package EA-MC, developed by C. Rubbia and his group at CERN. The code offers treatment of both high-energy particle interactions and low-energy neutron transport with a sophisticated method based on a full Monte Carlo simulation, together with the option of utilising different modern nuclear data libraries.

[1] University of Pavia, Italy

[2] Department of Radiation Sciences, Uppsala University, Sweden

[3] Emerging Energy Technologies, CERN, Switzerland

1 Introduction

Accurate neutron cross section information is a fundamental premise for the 3D Monte Carlo neutronic calculations that are made in order to determine the parameters of a nuclear reactor core. The various cross section libraries, however, show significant differences between their respective cross section data, in particular for intermediate neutron energies (~1 keV). In the case of neutronic calculations on transmutation systems, which are designed to operate with neutrons of intermediate to high energy, the issue becomes of significance. Utilisation of different cross section data causes deviations that are clearly larger than the statistical variations. The analysis thus aims to pinpoint the most problematic isotopes and reaction channels, which are responsible for the discrepancies in the main neutronic parameters. The results consequently indicate which isotopes are of high priority to the on-going neutron cross section measurement campaigns, such as the n_TOF experiment [1] presently being conducted at CERN.

2 The EA-MC Code Package

EA-MC [2] is a general geometry, "point-energy", Monte Carlo code which stochastically calculates the distribution of neutrons in three-dimensional space as a function of energy and time. The neutron data are derived from the latest nuclear data libraries [3]: ENDF/B-VI (USA), JENDL-3.2 (Japan), JEF-2.2 (Europe), EAF-4.2 (Europe), CENDL-2.1 (China), EFF-2.4 (Europe) and BROND-2 (Russia). The user has the option to utilise individual libraries or the CERN compilation of nuclear data, JAR-95. For each nuclide in JAR-95, one evaluation out of those available has been selected on the basis of a systematic comparison [4]. The selection was done isotope per isotope according to the evaluation of the resonances and the number of reaction cross sections. When both the resonance region and the number of cross sections evaluated were similar, the most recently evaluated cross section was selected. **Figure 1** gives an illustration of the element content in the EA-MC database.

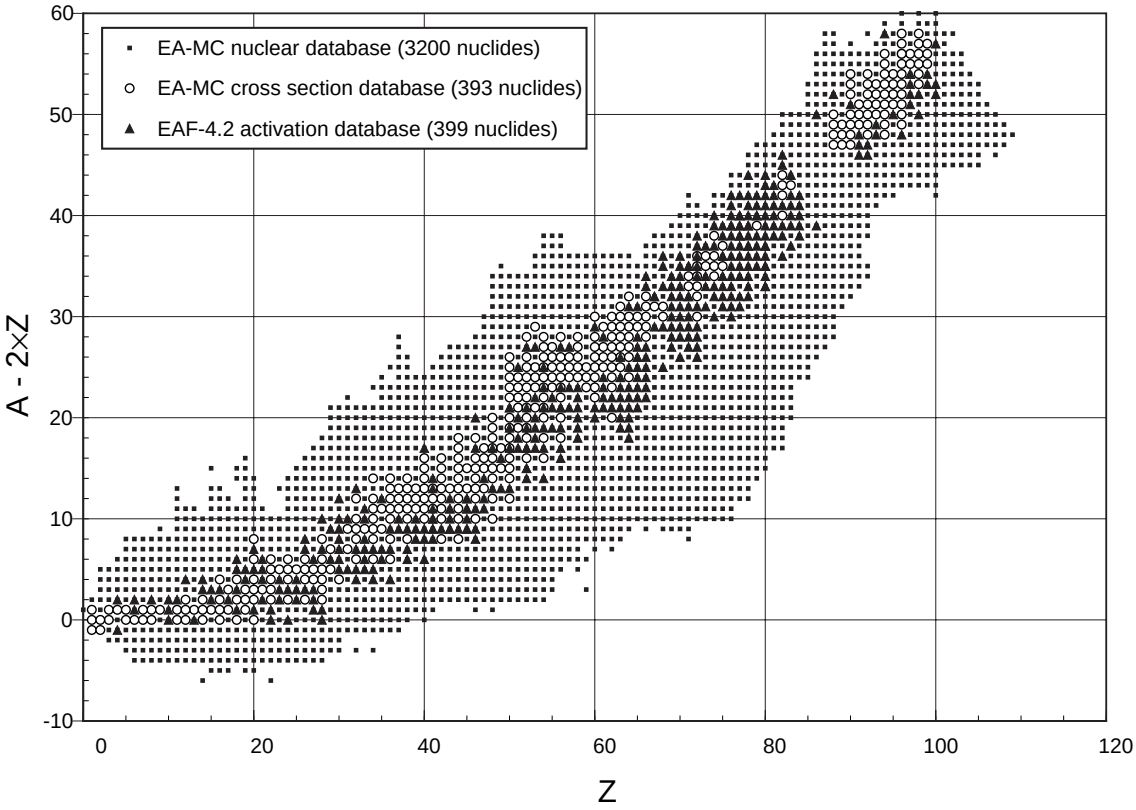

Figure 1. Summary of the element content in the EA-MC nuclear database, illustrated by a plot of A – 2Z vs Z, showing the larger extent of the EA-MC database.

The general architecture of the EA-MC code is shown in **Figure 2**. The geometrical description is first automatically translated into FLUKA's combinatorial geometry, and the high-energy particle transport is carried out [5,6]. Neutrons are transported down to 20 MeV and then handed over to EA-MC which continues the transport. The EA-MC code is designed to run both on parallel and scalar computer hardware. A common initialisation section is followed by a parallel phase where every CPU runs an independent simulation with the same initialisation data. A parallel analysis program collects the results and calculates the standard deviation among the different CPUs. This gives an estimate of the statistical fluctuations [7].

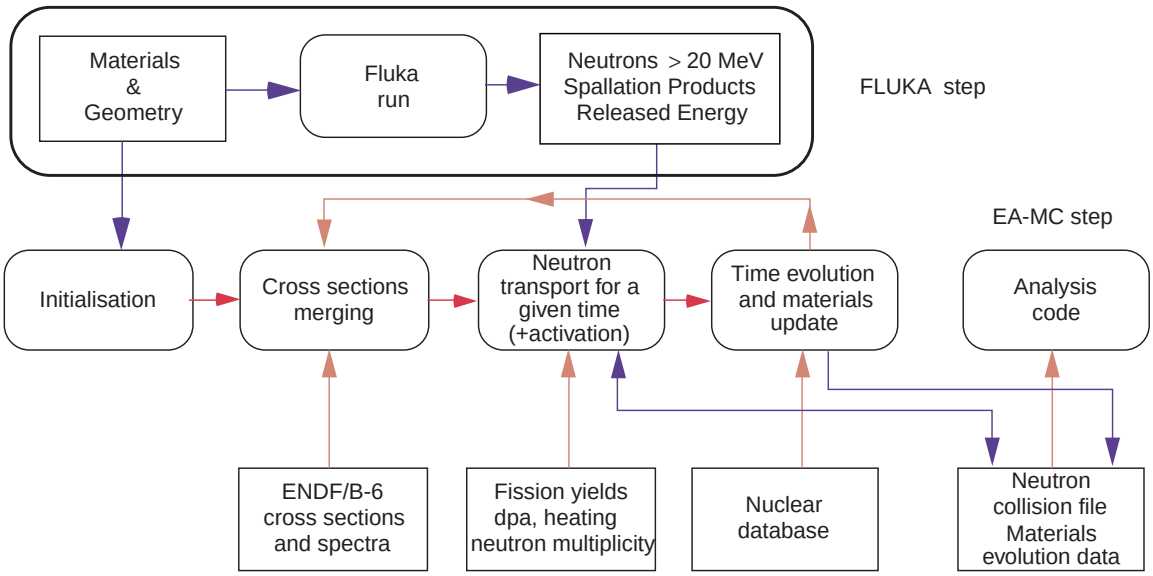

Figure 2. General architecture of the EA-MC Monte Carlo simulation of neutron transport and element evolution.

3 Principles and Requirements for ADS

3.1 Precision and Validation of Computational Models

In order to validate the computational methods that have been developed for calculations on source-driven subcritical systems, higher accuracy in the neutron cross section databases is required [8]. A measure of the general precision can be obtained from the uncertainty in reactivity per cycle, $\Delta\rho$/cycle, since safety margins and accelerator current demands will both be taken into account here. The precisions aimed at should be the same as for critical cores: ±10 pcm for UO_2 and ±4 pcm for MOX. Hence, the nuclides and reactions owning properties that affect the overall neutronics significantly have to be determined, as well as their respective importance in order to produce guidelines for the required accuracy.

The OECD NEA High Priority Nuclear Data Request List (HPRL) provides the cross sections that are considered of importance: For structural materials and coolant, inelastic scattering and (n,xn) in Fe, Cr, Ni, Pb, Bi, W are listed (should be known to an accuracy of ±5% to ±10%); For fission products, the capture cross

section of ^{99}Tc, ^{129}I, ^{131}Xe, ^{133}Cs, ^{135}Cs, ^{149}Sm, ^{151}Sm (±10%). Concerning the primary actinides, further precision is needed for the capture cross section of ^{232}Th, ^{233}U, ^{235}U, Pu-isotopes in the energy range from 1 eV to 500 keV (typically ±10%); For the inelastic scattering of ^{232}Th and ^{238}U (±5%), ^{239}Pu (±10%) and ^{240}Pu (±5%); For the fission cross sections of ^{232}Th and ^{238}U above 500 keV (typically ±10%), ^{233}U, ^{235}U, ^{239}Pu and ^{241}Pu in the energy range 1 eV to a few MeV (±1% to ±5%); The fission product yields of mass chains 92 to 140 for ^{233}U, ^{235}U and ^{239}Pu; and for the delayed neutron yields of ^{232}Th and ^{238}U (±3%), Pu-isotopes (±3% to ±7%), ^{237}Np and ^{241}Am (±5%). In the case of minor actinides, improved data are requested for capture, fission, inelastic scattering, (n,2n), fission neutron spectra, delayed neutron yields and spontaneous fission half-lives of ^{237}Np, ^{238}U, ^{241}Am, ^{243}Am and ^{244}Cm (typically a precision of ±10%).

3.2 The Energy Amplifier Demonstration facility

The Energy Amplifier Demonstration Facility [9] (EADF) was chosen as the basis for the principal part of the cross section sensitivity analysis, since the goal was to study the cross section data effects in a realistic and advanced system. The key objective of the EADF, in a first approximation, is to demonstrate the technical feasibility of a fast neutron operated accelerator-driven system cooled by molten lead-bismuth eutectic (LBE) and in a second phase that of incinerating TRUs and long-lived fission fragments while producing energy.

As in the case of the Energy Amplifier's conceptual design [2], the EADF core consists of an annular structure immersed in molten lead-bismuth eutectic which serves as primary coolant and spallation target (cf. **Figure 3**). The central annulus contains the spallation target unit which couples the proton accelerator to the sub-critical core. The core is arranged in a honeycomb-like array forming an annulus with four coaxial hexagonal rings of fuel sub-assemblies. The fuel core is itself surrounded by an annular honeycomb-like array of four rings of dummy sub-assemblies, which are essentially empty ducts. The detailed design of the EADF reference configuration has been developed in cooperation with Ansaldo Nucleare [9].

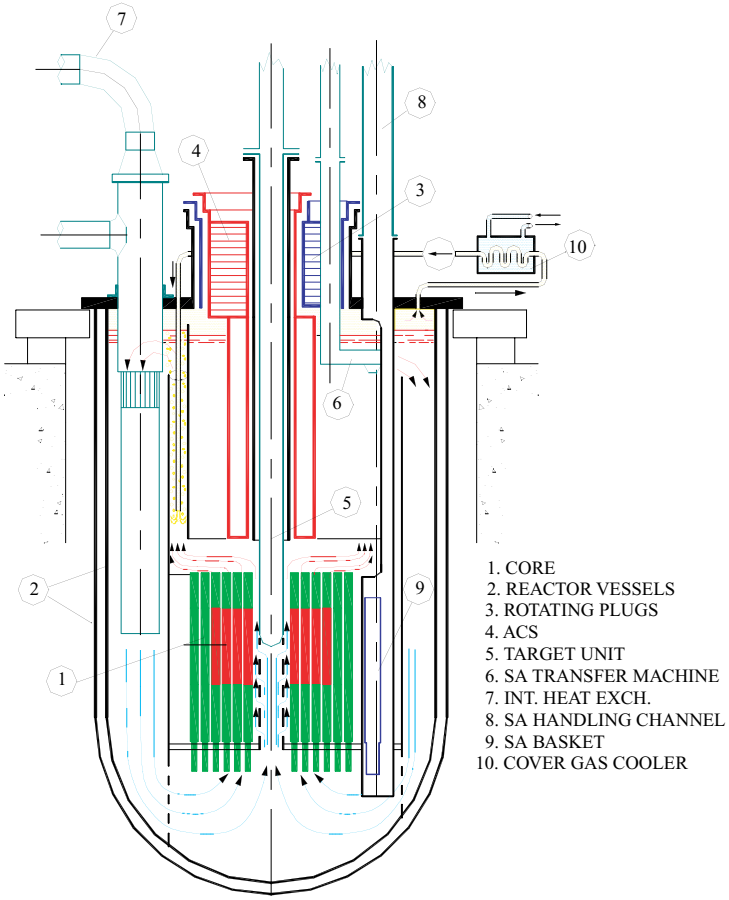

Figure 3. Schematic view of the EADF reactor system assembly.

4 Neutronic Analysis with Different Cross Section Libraries

The IAEA ADS Neutronic Benchmark (Stage 1) [8] showed that there are significant weaknesses concerning the cross sections relevant to ADS calculations. Some of the results are commented. Due to a lack of covariance data for different nuclides in several of the major neutron cross section libraries, a special approach is applied in the following sensitivity study performed. The strategy is to examine the neutron balance in different regions of the device first and thus pin-pointing critical regions. Finally, the isotopes and reaction channels causing serious discrepancies between calculations made with different libraries,

are isolated. To further develop the subject, some of the differences between the one-group cross sections of two of the libraries are highlighted.

4.1 IAEA ADS Neutronic Benchmark (Stage 1)

The aim of the IAEA ADS Neutronic Benchmark (Stage 1) was a verification of reactivity burnup swing and of certain reactivity effects for a fast spectrum ^{233}U-^{232}Th fuelled ADS driven by an external spallation neutron source at different subcriticality levels. A comparison between different nuclear data libraries unveiled large discrepancies, in particular when comparing the JEF-2.2 library and JAR-95 [4] a systematic underestimation of k_{src} of the order of 0.02 (2000 pcm) was noted for the part of JEF-2.2 (see **Figure 4**). A difference of this order requires an increase of the initial concentration of ^{233}U by 4% to compensate for the lack of reactivity in the JEF-2.2 case. This has negative effects on the dynamical properties and the safety margins of the system [8].

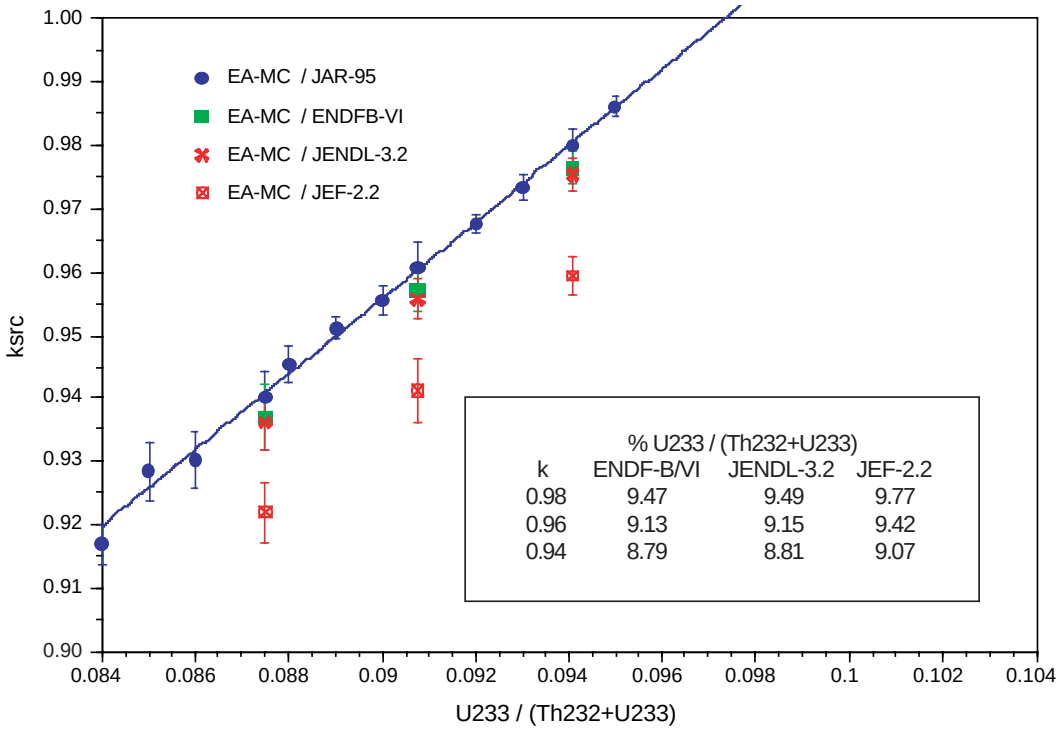

Figure 4. Comparison of the variation of k_{src} as a function of the concentration of ^{233}U for different nuclear data libraries.

A closer examination of the neutron reaction balance revealed that the ratio of fissions in ^{233}U to captures in ^{232}Th was 0.79 with JAR-95 whereas it was only 0.76

with JEF-2.2, thus affecting the burnup calculations. Upon studying the neutron spectra it was established that the energy range from 1 keV to 5 MeV was central in this simulation, and as can be perceived from **Figure 5**, the capture cross section of ^{232}Th differs to a large extent here, even exhibiting a discontinuity at precisely 50 keV.

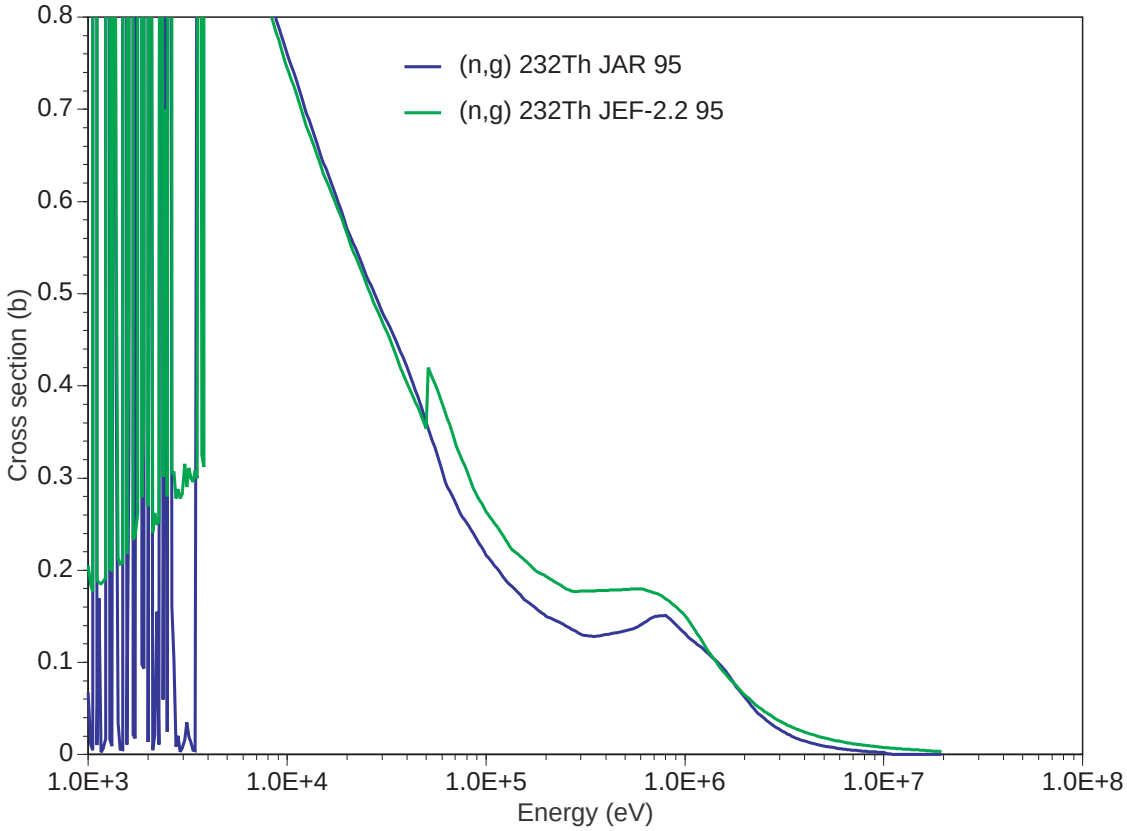

Figure 5. (n,γ) cross section for ^{232}Th from JEF-2.2 and JAR-95.

The reason is the background cross section being set to 0 in the region of unresolved resonances, which extends from 3.94 keV to 50 keV, while the background cross section resumes after 50 keV, producing a background mismatch at this point. Therefore a jump corresponding to 20% in the cross section value is observed at this point. The result is an overestimation of the capture cross section of ^{232}Th, which eventually is responsible for the mentioned underestimation of k_{src}.

4.2 Neutron Balance and Cross Section Data Effect for Particular Nuclides

The effect of the cross section data discrepancies on the calculated main parameters of the EADF are easily seen in **Table 1**, which presents the source multiplication constant for different libraries. A difference of the order 0.02 (2000 pcm) in k_{src} is noted between the JAR-95 (henceforth referred to as "JAR") and JENDL-3.2 ("JENDL") cases, whereas it is 0.005–0.010 (500–1000 pcm) between the JAR and ENDF/B-VI ("ENDF") cases (cf. Section 5.1). In other words, the accuracy of the k_{src} calculation is between two to three orders of magnitude off from the aims presented in Section 3.1! The explanation is to be found in the neutron energy spectra and in the cross section data libraries.

Table 1. Neutron cross section data effect in k_{src}.

	JAR	ENDF/B-VI	JENDL-3.2
$UPuO_2$	0.96403	0.95883	0.93937
(error)	±0.00070	±0.00094	±0.00106
$\Delta k/k$ in pcm		*-539*	*-2558*
ThPuO	0.96260	0.94945	0.94526
(error)	±0.00102	±0.00109	±0.00088
$\Delta k/k$ in pcm		*-1366*	*-1801*

4.3 Spectrum Effect

The neutron spectra are essentially similar between the U and Th fuel types when the same library is used[1]. However, when different libraries are used, systematic discrepancies of 10% to 30% can be observed between the spectra in the energy range from 10^4 to 10^6 eV. The spectrum effects for different materials are illustrated in **Figures 6–8**, which show the neutron energy spectra obtained with different libraries. The two respective spectral differences between the comparison libraries (JENDL and ENDF) and the reference library (JAR) are also

[1] Due to the similarity in neutron energy spectra for the two fuel types, the discussion in this study will be limited to the spectra obtained with uranium fuel.

plotted in these figures. It should be noted that the scaling of the coordinate axes varies from figure to figure, since this is necessitated by the fact that the flux magnitudes and the relevant energy ranges differ between the materials.

From **Figure 6** it is seen that ENDF and JAR exhibit closely similar neutron spectra in the uranium fuel. JENDL, on the other hand, distinguishes itself with a neutron flux roughly 20% lower than JAR between 10^5 and a little over 10^6 eV of neutron energy. Thus, the JENDL case can be expected to show a deficit in both the amount of fast fissions and the number of (n,xn) reactions produced in the fuel (cf. Section 4.2, **Table 4**). Although a slight excess in the flux (~10%) can be noted for JENDL in the energy range stretching from roughly 10^4 to 10^5 eV, it will not increase the multiplicative (n,xn) process in the fuel, since the threshold for these reactions lies around 10^6 eV. On the other hand, it may to some extent compensate the negative effects expected in the case of fast fission[2].

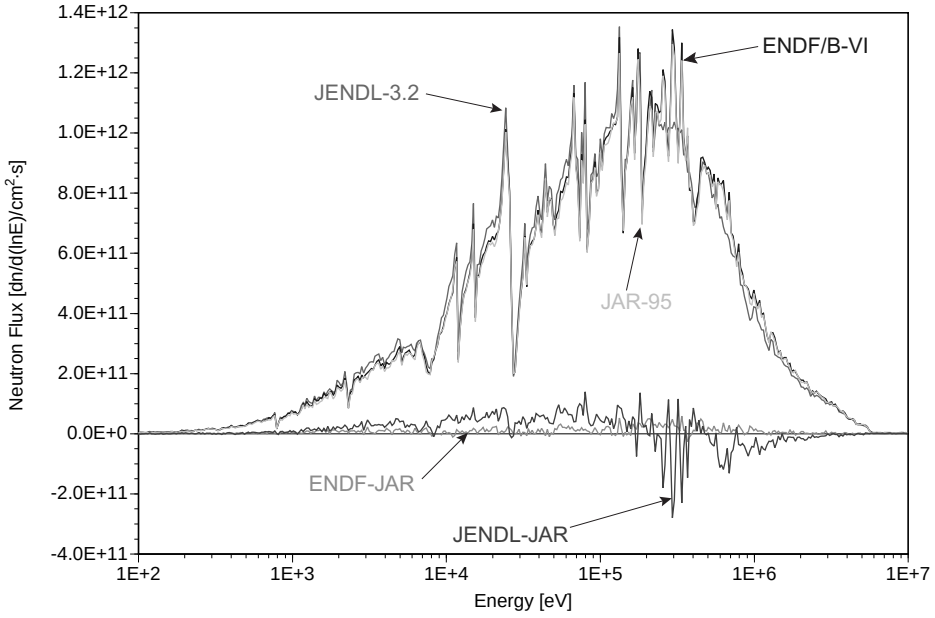

Figure 6. Discrepancies between nuclear data libraries for the neutron energy spectra in the uranium fuel.

[2] For fissile nuclides, the fission cross section is higher between 10^4 and 10^5 eV than between 10^5 and 10^6 eV, while the opposite is true for the fertile ones. However, the capture cross section is also higher for both nuclide types between 10^4 and 10^5 eV.

The flux differences in the LBE coolant (cf. **Figure 7)**, show similarities to the ones seen for the fuel materials previously. ENDF shows only minor differences from JAR (10% excess), while for JENDL significant differences of 30% lower flux are noted in the energy range from 10^4 to 10^6 eV, and then most pronouncedly between 10^5 and 10^6 eV. The comparatively smaller spectrum effect in the fuel (cf. **Figure 6**) is due to the fact that most of the neutrons are born there and still retain their energy while in the fuel material. In the coolant neutrons are generally propagated for longer distances and anomalies in the cross sections consequently carry a larger impact on the neutron energy spectrum.

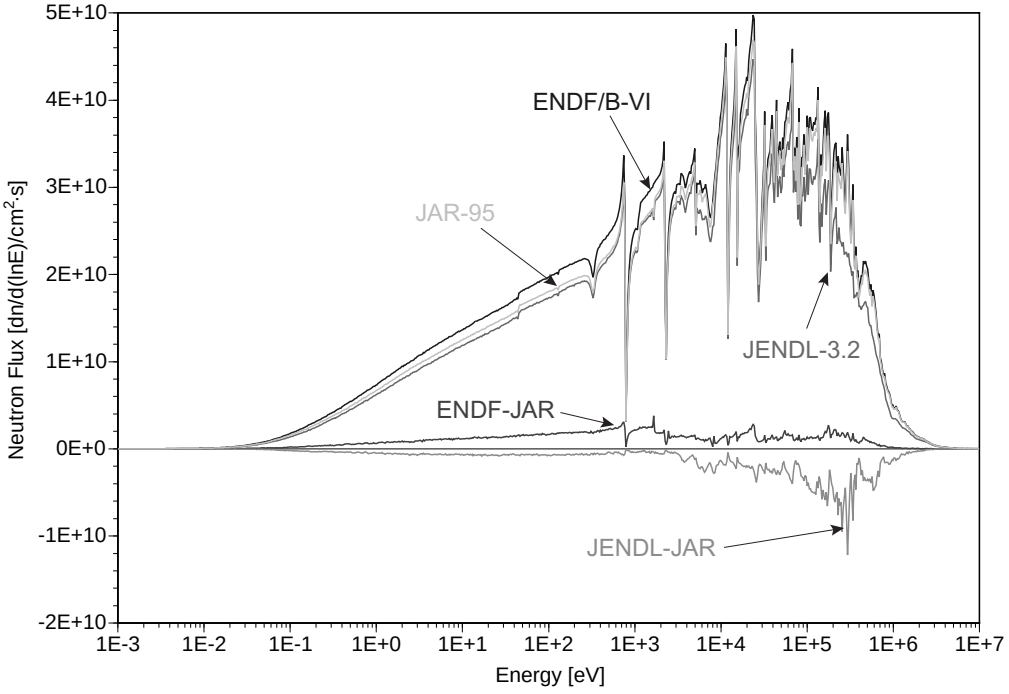

Figure 7. Discrepancies between nuclear data libraries for the neutron energy spectra in the LBE coolant.

An explanation to the anomalies seen between the neutron energy spectra of different libraries is possibly found in the elastic cross section of lead. Due to its large volume and the fact that elastic scattering is the most occurrent process in the material, this cross section is of particular importance to the neutron energy distributions in the whole system. Upon comparison, it is found that the JAR and

JENDL evaluations of the elastic cross sections in lead differ significantly[3]. As an example, the discrepancy in the elastic cross section of the most important lead isotope, ^{208}Pb, is presented in **Figure 8**.

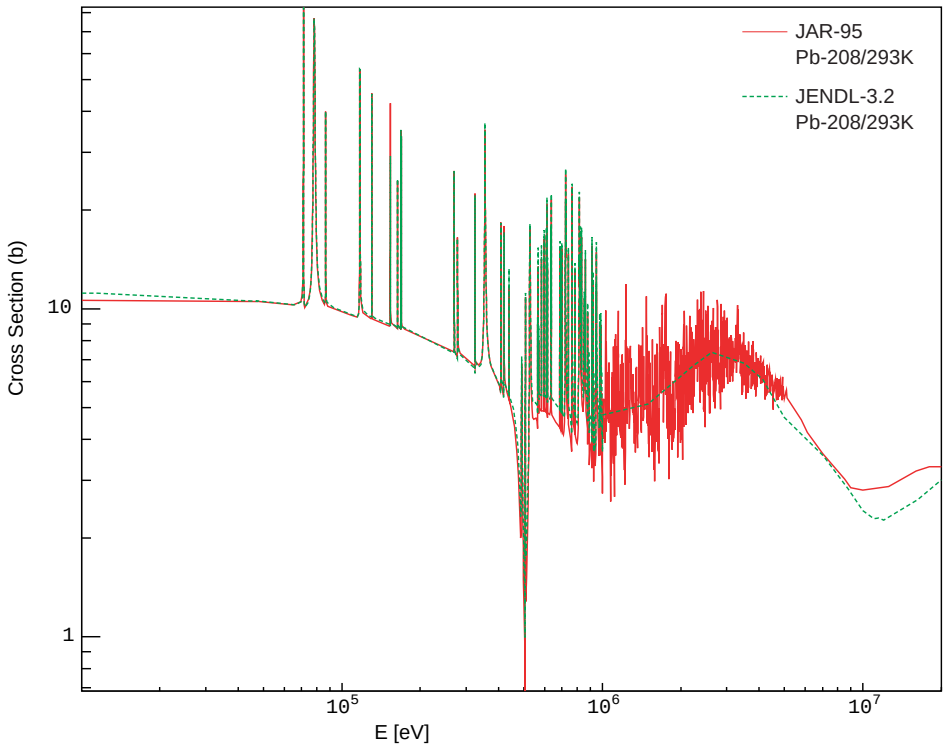

Figure 8. Discrepancy between JAR and JENDL in the elastic neutron cross section of ^{208}Pb.

In JENDL, the elastic cross section seems to be set higher from about 5×10^5 eV up to a little above 10^6 eV. In addition, the resonances above 10^6 eV are unresolved, whereas in JAR, they are accounted for up to 5×10^6 eV. For the other two relevant lead isotopes, ^{206}Pb and ^{207}Pb corresponding differences were found, with the unresolved resonance region starting even at lower energies (from approximately 5×10^5 eV). Disregarding the resonance structure in this energy range necessarily alters the elastic scattering properties of the LBE coolant, and

[3] ^{209}Bi was also checked, but here the differences were of less significance.

so the significant spectrum effect seen in **Figure 7** can be traced back to this difference in the elastic cross section of the lead isotopes.

From **Figure 9**, it can be noted that the fluxes obtained with ENDF and JAR are closely similar in the cladding. The spectrum effect between JENDL and JAR primarily consists of an excess neutron flux in the range from 10^4 to 10^6 eV. A higher flux suggests a lower cross section in the concerned energy range, which can only derive from the elastic and non-elastic cross sections being estimated lower in the cladding materials.This is mainly due to the neglect of resonances in JENDL for energies higher than 3×10^5 eV – from these energies an averaging effect in the cross sections is seen (cf. **Figure 10**), at points the difference between JENDL and JAR reaching the same order of magnitude as the flux itself.

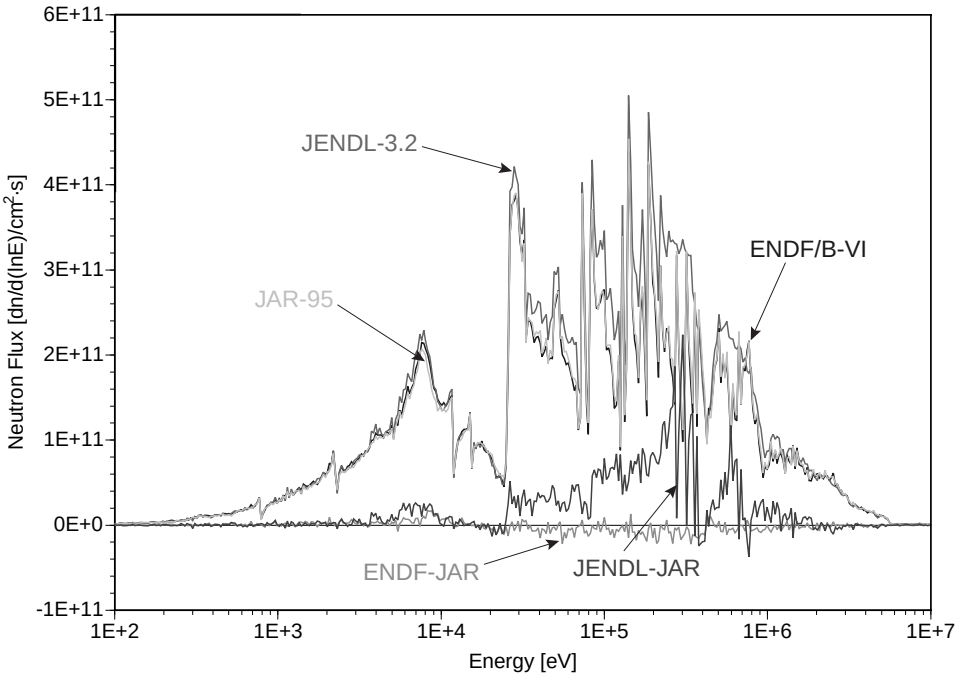

Figure 9. Discrepancies between nuclear data libraries for the neutron energy spectra in the cladding.

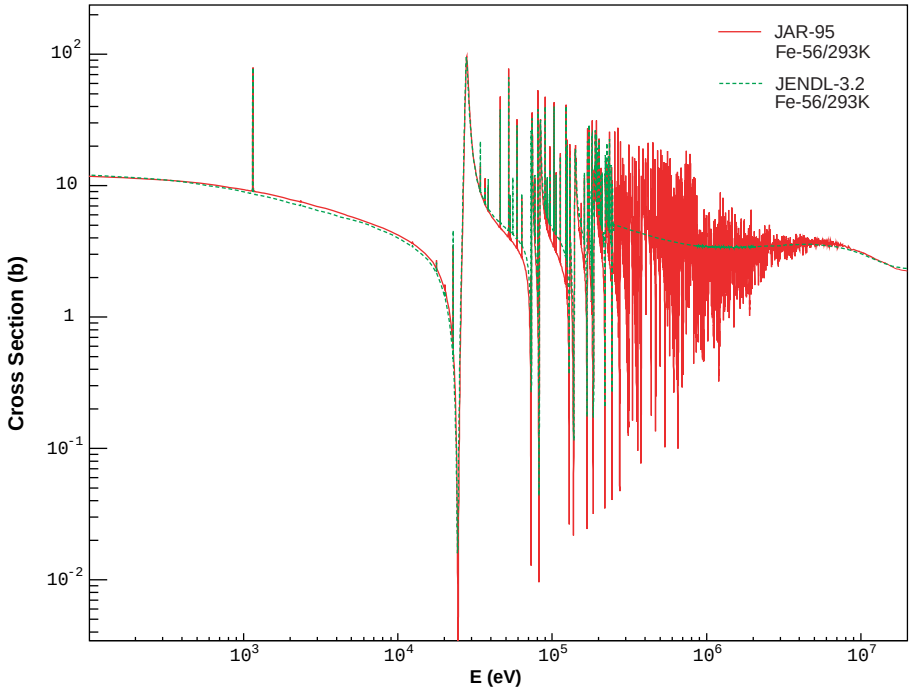

Figure 10. Discrepancy between JAR and JENDL in the total neutron cross section of ^{56}Fe.

4.4 Neutron Balance

The conflict between the libraries is further demonstrated upon examining the fuel core neutron balance for the uranium and thorium MOX fuels shown in **Tables 2** and **3**, respectively. Reactions are classified as either "capture", "fission", "n,xn" or "other" (n,p; n,d; n,np; n,2p...) in each material examined (fuel, coolant and cladding). The occurrence of each reaction is given as a relative percentage. Only reactions that contribute significantly to the neutron balance are listed. The columns headed by Δ_{JENDL} or Δ_{ENDF} contain the relative percentage differences between the cross section library in question and JAR (reference). In the tables, the relative percentage difference is highlighted when greater than 2% and when statistics are sufficient. The Δ_{JENDL} or Δ_{ENDF} value is omitted when the occurrence of the reaction is low.

Table 2. Neutron balance in the fuel core with (U-Pu)O_2 fuel.

Fuel	JAR	JENDL	Δ_{JENDL}	ENDF	Δ_{ENDF}
Captures	51.79%	53.72%	***+3.74%***	52.14%	*+0.67%*
Fissions	47.67%	45.79%	***-3.93%***	47.28%	*-0.82%*
n,xn	0.34%	0.30%		0.34%	
Coolant	JAR	JENDL	Δ_{JENDL}	ENDF	Δ_{ENDF}
Captures	61.29%	62.80%	***+2.46%***	58.67%	***-4.28%***
n,xn	38.06%	36.85%	***-3.17%***	40.62%	***+6.73%***
Cladding	JAR	JENDL	Δ_{JENDL}	ENDF	Δ_{ENDF}
Captures	89.96%	92.74%	***+3.08%***	90.24%	*+0.31%*
n,xn	4.44%	3.10%	***-30.03%***	4.54%	***+2.42%***
Others	5.60%	4.16%	***-25.74%***	5.22%	***-6.84%***

Table 3. Neutron balance in the fuel core with (Th-Pu)O_2 fuel.

Fuel	JAR	JENDL	Δ_{JENDL}	ENDF	Δ_{ENDF}
Captures	52.86%	54.36%	***+2.84%***	53.84%	*+1.84%*
Fissions	46.47%	45.05%	***-3.05%***	45.41%	***-2.27%***
n,xn	0.48%	0.41%		0.51%	
Coolant	JAR	JENDL	Δ_{JENDL}	ENDF	Δ_{ENDF}
Captures	60.47%	61.44%	*+1.61%*	58.28%	***-3.62%***
n,xn	38.85%	38.23%	*-1.60%*	41.07%	***+5.72%***
Cladding	JAR	JENDL	Δ_{JENDL}	ENDF	Δ_{ENDF}
Captures	89.46%	92.33%	***+3.21%***	89.98%	*+0.58%*
n,xn	4.54%	3.31%	***-27.12%***	4.61%	*+1.49%*
Others	6.00%	4.36%	***-27.28%***	5.41%	***-9.76%***

For both types of fuel, similar trends are found for the examined reaction types; the Δ_{JENDL} or Δ_{ENDF} differ but to a small extent depending on fuel type. The tendency is that capture reactions appear to a larger extent for the JENDL case when compared with the reference. Instead the "neutron production" reactions, fission and (n,xn) are of less frequency than for the reference case. Although the most striking relative percentage differences (25% to 30%) arise for (n,xn) and other reactions in the cladding for both the U- and Th-based fuels, it should be

noted that these reactions occur to a low relative percentage compared to the capture reactions. More importantly, an excess of 2% to 4% of capture reactions is seen with JENDL in all materials and for both fuel types. This effectively reduces the reactivity of the core, and an underestimation of k_{src} will follow.

The effect is further enhanced by the fact that two multiplicative processes, fissions in the fuel and (n,xn) in the coolant, show a result 2% to 4% lower compared with the reference. Concerning the fuel, the ENDF case behaves similarly to the JENDL case, although the differences are less pronounced, around 1% to 2%. ENDF distinguishes itself from the other two libraries in the coolant materials due to a 6% to 7% higher relative occurence of (n,xn) reactions and a 4% lower of capture than in the reference case. This multiplicative effect in the coolant compensates to some extent for the lack of reactivity in the fuel relative to JAR. In the cladding, the behaviour resembles the reference, except for a deficit in "other" reactions and a small surplus in captures and (n,xn).

The fission to capture ratio for U-based fuel with JAR is 0.92, 0.85 with JENDL and 0.91 with ENDF. With Th-based fuel, JAR yields 0.88, JENDL 0.83 and ENDF 0.84. Hence, the nuclides in the fuel need to be studied in detail. **Tables 4** and **5** present the neutron balance for some important nuclides in which notable discrepancies arise. The same notation is used as in the previous tables.

The results in **Tables 4** and **5** verify the pattern seen previously for JENDL. Capture reactions occur to a higher degree, from 0.5% to 25% higher than with the other two libraries, while 1% to 11% fewer fissions are produced. As was expected, the libraries seem to agree rather well for the well-known ^{235}U. However, poor agreement is generally found for the other central nuclides. The largest disagreements are seen for the U-based fuel, for fission in ^{240}Pu (-16%) and ^{238}U (-11%), and for capture in ^{241}Pu (25%). A glance at the fuel tables in **Tables 2** and **3** verifies this fact; the capture/fission discrepancy is indeed larger for U-based fuel. For ENDF, the results are also in agreement with what was seen previously. The largest deviations from reference are found for fission in ^{232}Th (-7.5%) and capture in ^{241}Pu (5%). For ^{235}U and ^{239}Pu, even slightly more fissions and fewer captures occur than in the reference case.

Table 4. Reactions in important nuclei in the (U-Pu)O_2 fuel.

^{235}U	JAR	JENDL	Δ_{JENDL}	ENDF	Δ_{ENDF}
Capture	21.94%	22.28%	*1.51%*	21.77%	*-0.79%*
Fission	77.91%	77.64%	*-0.35%*	78.17%	*0.33%*
N,xn	0.14%	0.09%		0.06%	
^{238}U	JAR	JENDL	Δ_{JENDL}	ENDF	Δ_{ENDF}
Capture	87.45%	88.81%	*1.56%*	87.70%	*0.29%*
Fission	11.70%	10.40%	***-11.13%***	11.37%	***-2.77%***
N,xn	0.85%	0.79%		0.92%	
^{239}Pu	JAR	JENDL	Δ_{JENDL}	ENDF	Δ_{ENDF}
Capture	21.99%	22.97%	***4.47%***	21.46%	***-2.40%***
Fission	77.98%	76.99%	*-1.27%*	78.50%	*0.67%*
N,xn	0.03%	0.04%		0.04%	
^{240}Pu	JAR	JENDL	Δ_{JENDL}	ENDF	Δ_{ENDF}
Capture	57.20%	63.89%	***11.70%***	57.65%	*0.79%*
Fission	42.71%	36.04%	***-15.62%***	42.30%	*-0.96%*
N,xn	0.08%	0.07%		0.04%	
^{241}Pu	JAR	JENDL	Δ_{JENDL}	ENDF	Δ_{ENDF}
Capture	13.05%	16.29%	***24.75%***	13.82%	***5.89%***
Fission	86.91%	83.63%	***-3.78%***	86.18%	*-0.84%*
N,xn	0.04%	0.09%		0.00%	

Table 5. Reactions in important nuclei in the (Th-Pu)O_2 fuel.

^{232}Th	JAR	JENDL	Δ_{JENDL}	ENDF	Δ_{ENDF}
Capture	95.79%	96.31%	*0.55%*	95.90%	*0.12%*
Fission	2.90%	2.64%	***-8.76%***	2.68%	***-7.50%***
N,xn	1.31%	1.04%		1.41%	
^{239}Pu	JAR	JENDL	Δ_{JENDL}	ENDF	Δ_{ENDF}
Capture	21.09%	22.00%	***4.28%***	20.44%	***-3.11%***
Fission	78.87%	77.97%	*-1.14%*	79.52%	*0.82%*
N,xn	0.03%	0.03%		0.04%	
^{240}Pu	JAR	JENDL	Δ_{JENDL}	ENDF	Δ_{ENDF}
Capture	55.52%	60.94%	***9.77%***	55.60%	*0.15%*
Fission	44.37%	38.92%	***-12.28%***	44.35%	*-0.05%*
N,xn	0.11%	0.13%		0.05%	
^{241}Pu	JAR	JENDL	Δ_{JENDL}	ENDF	Δ_{ENDF}
Capture	13.08%	15.21%	***16.28%***	13.69%	***4.67%***
Fission	86.88%	84.79%	***-2.41%***	86.28%	*-0.69%*
N,xn	0.04%	0.00%		0.02%	

The discrepancies seen in the neutron balances examined either originate from the spectrum effects seen earlier in Section 4.3, or arise from differences in the cross sections. For example, in JENDL the spectrum effect contributes with a reduction of the number of (n,xn) in the fuel and the coolant, and should correspondingly increase the (n,xn) in the cladding. Such an effect can *not* be distinguished in the cladding; the expected spectrum effect is rather cancelled by a comparatively even larger cross section discrepancy. In order to draw conclusions about which of the effects dominate, the cross sections have to be examined directly.

4.5 Comparison of One-Group Cross Sections in JAR and JENDL

The marked differences between JENDL and JAR, motivated a comparison of their one-group (1-g) cross sections. These were obtained by convoluting the neutron flux spectra of the materials of interest with pointwise cross section. In **Figure 11** the fission, capture and (n,2n) cross sections in the fuel materials are presented. Discrepancies larger than 10% are exhibited for capture and (n,2n) in ^{238}Pu, ^{240}Pu and ^{241}Pu; (n,2n) in ^{232}Th, ^{235}U, ^{242}Pu, ^{237}Np and ^{241}Am. The very large differences seen in the case of ^{238}Pu are far from the aim defined by the HPRL, typically 20% up to 20 MeV. However, ^{238}Pu appears in more modest quantities than the other nuclides and is mostly of interest from a waste transmutation point of view.

More remarkable is the poor cross section precision for the other nuclides, which appear in larger quantities in spent LWR fuel or play a more productive role in an ADS. From the graph it is seen that the general trend of lower fission cross sections and higher captures again is confirmed (cf. **Tables 2–5**). The particularly large relative percentage differences in (n,2n) should be considered from the perspective of its relatively low absolute value, being in the examined fuel materials 10^3–10^4 times lower than for capture: a small percentage excess in capture cross section will dominate a large one in the (n,2n) cross section. Hence, the deficit in (n,xn) in the reaction balances for the fuel in **Tables 2–5** is due to the excess of the capture cross section. In the fuel, the neutron flux was noted to be lower just below and above 1 MeV, (cf. **Figure 6** and the discussion around it), the threshold energy for (n,xn); this spectrum effect also contributes to the decrease of (n,xn) reactions.

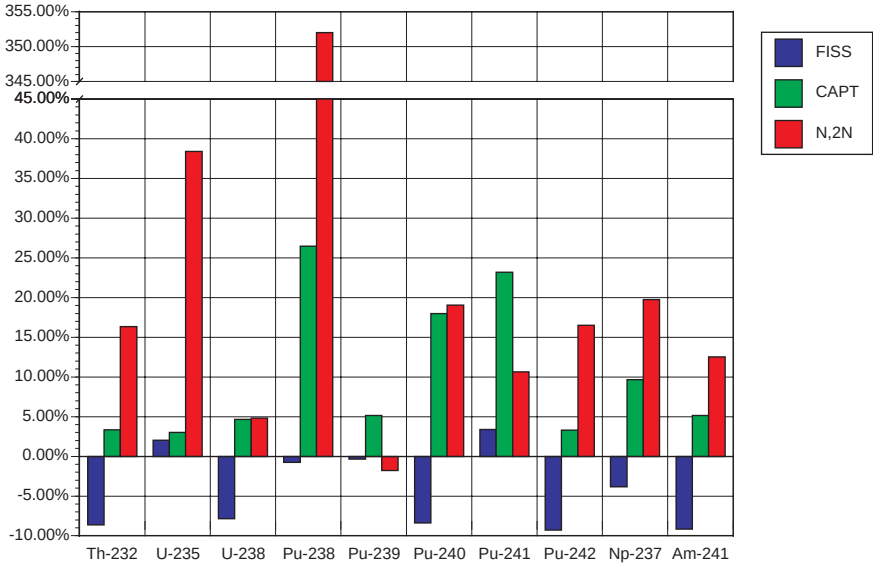

Figure 11. Relative difference between JAR and JENDL 1-g fission, capture and (n,2n) cross sections for fuel materials. (JAR as reference)

Figure 12 shows the differences for elastic and inelastic scattering cross sections in the fuel. The most notable differences are seen for both cross sections in ^{238}Pu and ^{241}Pu, but also over 10% differences are found for inelastic scattering in ^{235}U, ^{240}Pu and ^{241}Pu.

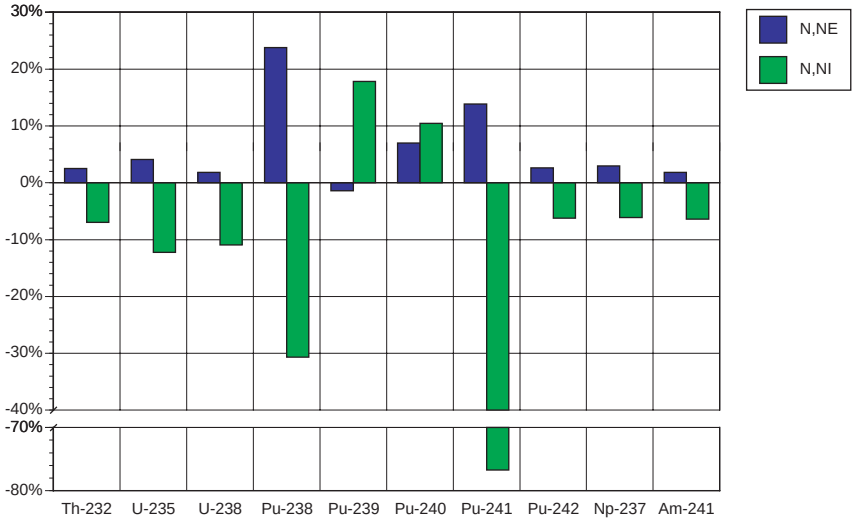

Figure 12. Relative difference between JAR and JENDL 1-g (n,n) and (n,n') cross sections for fuel materials.

Capture, (n,2n), elastic and inelastic scattering cross sections have all been included in **Figure 13** exhibiting their relative difference in cladding materials. ^{55}Mn is the only nuclide for which all the cross sections agree to an accuracy of 10%. The Fe isotopes have these cross sections generally determined to an accuracy between 10% and 20%, which is a factor 2 or more than what is specified on the HPRL. If the most abundant isotopes are considered, ^{56}Fe, ^{52}Cr and ^{54}Fe, it can be concluded that the discrepancy in capture again will dominate the one in (n,2n), and even more so, since in two of these nuclides actually register a deficit in the (n,2n) 1-g cross section (for ^{56}Fe cf. discussion on **Figure 10**). The results are in good agreement with the reaction balances in the cladding in **Tables 2** and **3**.

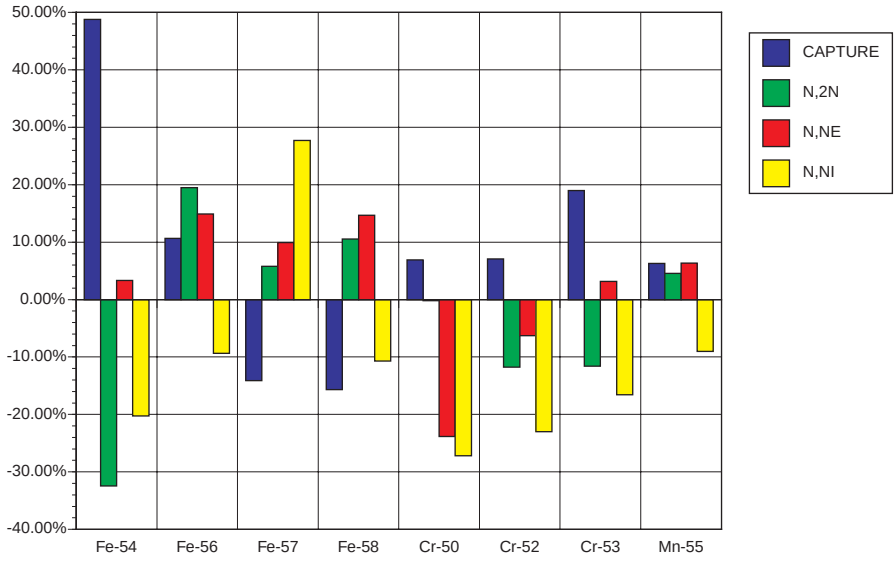

Figure 13. Relative difference between JAR and JENDL 1-group capture, (n,2n), (n,n) and (n,n') cross sections for cladding materials.

Figure 14 presents the relative difference between capture, (n,2n), elastic and inelastic scattering cross sections in the coolant. Differences are in general over 10% for (n,2n), inelastic scattering and capture for the Pb isotopes. The libraries are seen to agree better for ^{209}Bi, although (n,2n) and inelastic scattering show a variation of close to 10%. The elastic scattering cross section differences stay around or below 5%. The fact that JENDL generally lists *higher* (n,2n) 1-g cross sections, but still gets a *lower* occurrence of (n,xn) in **Tables 2** and **3**, is explained

by the spectrum effect (seen in Section 4.3, **Figure 7**) affecting the 1 MeV (n,xn) threshold region.

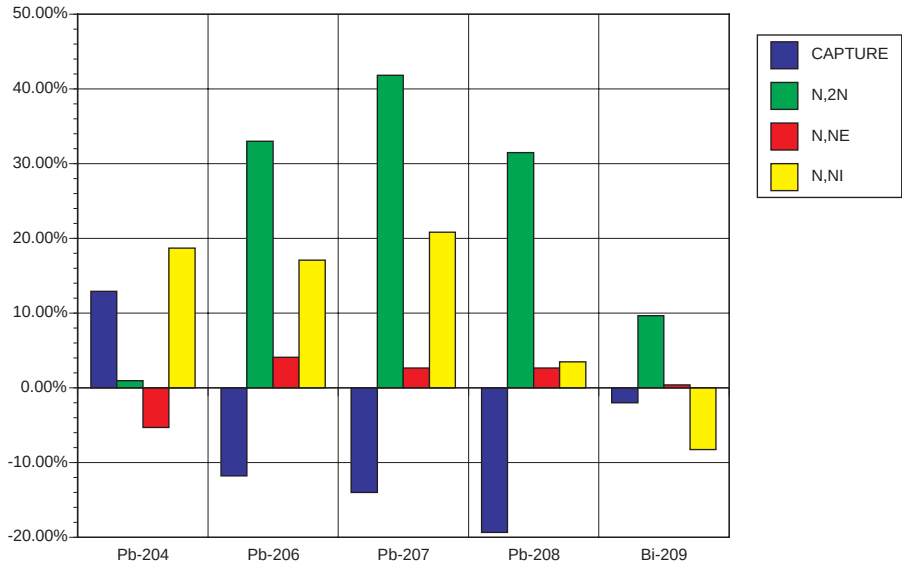

Figure 14. Relative difference between JAR and JENDL 1-group capture, (n,2n), (n,n) and (n,n') cross sections for coolant materials.

5 Conclusion and Discussion

Both for IAEA ADS Neutronic Benchmark (Stage 1) and the EADF cross section sensitivity analysis, discrepancies of roughly 0.02 (2000 pcm) in k_{src} were seen between different nuclear data libraries. Spectrum effects of generally 10% to 30% were noted in the energy range 10^4–10^6 eV for JENDL consisting of a softening effect in fuel and coolant, and a hardening effect in the cladding. For the ENDF library only minor spectrum effects (≤10%) were seen. The effect manifested itself in the resulting neutron balance mainly as a deficit of (n,xn) reactions in the coolant.

Concerning fuel materials, further measurements are of importance for the fission cross section (fast) for ^{232}Th, ^{238}U, ^{240}Pu and ^{242}Pu. In ^{238}Pu, ^{240}Pu and ^{241}Pu, more precision is required for capture reactions. The inelastic cross section is seen to differ between libraries especially for ^{238}Pu, ^{239}Pu, ^{240}Pu and ^{241}Pu. Elastic scattering appears well determined except for ^{238}Pu and ^{241}Pu. The (n,xn) cross

section seem to be determined with a poor accuracy for most of the examined nuclides, even for ^{235}U. This partly stems from the fact that the magnitude of the (n,xn) cross section is low relative to other ones.

In the cladding material, the Fe isotopes are of most importance, and in general, measurements are needed of the capture cross section. ^{54}Fe that occurs to 6% in natural iron shows a 50% discrepancy. Further precision also seems to be needed in the other cross sections examined for Fe, possibly also for ^{52}Cr.

The coolant materials are distinguished by poor accuracy in capture, (n,2n) and inelastic cross sections for the Pb isotopes. This is remarkable, since (n,xn) in the Pb coolant play an important role in an ADS and since as a coolant material is found in abundance. ^{209}Bi only shows a larger discrepancy for (n,2n).

It should be noted that the relative differences between the libraries do not represent the absolute uncertainty for the reaction in the respective nuclide, it is only a measure of how much the libraries differ. The "true" uncertainty is not taken into consideration in this text; the recommendations are given according to the differences between the libraries compared.

The one-group cross section study indicated that some nuclides that now were omitted need to be investigated further in the context of the EADF. A full analysis with a cross section sensitivity-uncertainty code utilising cross section data covariance files is also foreseen.

6 Acknowledgements

We thank the doctoral students who participated in the present study and initiated many discussions on the subject. The n_TOF Collaboration and, in particular, P. Pavlopoulos, F. Käppeler, N. Colonna, and H. Leeb are aknowledged for their encouragement and support to perform this analysis.

7 References

[1] "Proposal for a Neutron Time of Flight Facility," CERN/SPSC 99-8, CERN (1999).

[2] C. Rubbia et al., "Conceptual Design of a Fast Neutron Operated High Power Energy Amplifier," CERN/AT/95-44 (EET), Emerging Energy Technologies, SL Division, CERN (1995).
See also Y. Kadi, "Neutronic Analysis of the Energy Amplifier Demonstration Facility using the EA Monte Carlo Code," EET Internal Note 2000-009, Emerging Energy Technologies, SL Division, CERN (2000).

[3] OECD/NEA, Data Bank (Issy-les-Moulineaux, Paris, France, 1994).

[4] M. Cobo et al., "Notes on the Study of the Most Reliable Neutron Cross Section Data," CERN Internal Report, CERN/AT/ET 95-035, Geneva, August 15, 1995.

[5] A. Fassó, A. Ferrari, J. Ranft, P. R. Sala, J. M. Zazula, "A Comparison of FLUKA Simulations with Measurements of Fluence and Dose in Calorimeter Structures," *Nucl. Instrum. Methods Phys. Res., A,* **332** (1993), pp.459 – 468, also, CERN/TIS-RP/93-2/PP, CERN (1993).

[6] A. Fassó, et al., "Intermediate Energy Nuclear Data: Models and Codes," *Proceedings of a Specialists' meeting,* Issy-les-Moulineaux, Paris, France, 30 May – 1 June 1994, p.271.

[7] S. Atzeni, Y. Kadi, C. Rubbia, "Statistical Fluctuations in Monte Carlo Simulations of the Energy Amplifier," CERN/LHC/EET 98-004, CERN (1998).

[8] F. Carminati, Y. Kadi, "ADS Neutronic Benchmark (stage 1)," CERN/ET/Internal Note 98-005, *IAEA Technical Committee Meeting on Feasibility and Motivation for Hybrid Concepts for Nuclear Energy Generation and Transmutation,* CIEMAT, Madrid, Spain, 17 – 19 September 1994.

[9] Ansaldo Nucleare, "Energy Amplifier Demonstration Facility Reference configuration: Summary Report," EA-B0.00-1-200 - Rev. 0, ANSALDO Nucleare (1999).

COMPARATIVE ASSESSMENT OF THE TRANSMUTATION EFFICIENCY OF PLUTONIUM AND MINOR ACTINIDES IN FUSION/FISSION HYBRIDS AND ADS

Marcus Dahlfors
Department of Radiation Sciences
Uppsala University
Uppsala, Sweden

Yacine Kadi
Emerging Energy Technologies
CERN, European Organisation for Nuclear Research
Geneva,Switzerland

Abstract

A preliminary comparative assessment relevant to the transmutation efficiency of plutonium and minor actinides has been performed in the case of ANSALDO's Energy Amplifier Demonstration Facility based on molten lead/bismuth eutectic cooling, classical MOX-fuel technology and operating at 80 MW_{th}. The neutronic calculations presented in this paper are a result of a state-of-the-art computer code package, EA-MC, developed by C. Rubbia and his group at CERN. Both high-energy particle interactions and low-energy neutron transport are treated with a sophisticated method based on a full Monte Carlo simulation, together with modern nuclear data libraries. Detailed Monte Carlo transport calculations were performed for different types of external neutron sources: D-D and D-T fusion sources and proton induced spallation neutron sources. The fuel core was described on a pin-by-pin basis allowing for detailed scans of the main neutronic properties, e.g. neutron flux spectra and power density distributions.

Introduction

The Energy Amplifier Demonstration Facility (EADF) [1] is a hybrid system designed to be driven by an external source. The present design utilises a proton induced spallation neutron source for providing the external neutrons, but as such, the system is not limited to any particular choice of source as long as neutrons of suitable energy are provided. In this study, the neutronic properties of the reference spallation source driven EADF system has been compared to those of the system driven by two different alternative neutron sources: D-D and D-T fusion sources.

The EA-MC code package

EA-MC is a general geometry, "point-energy", Monte Carlo code which stochastically calculates the distribution of neutrons in three-dimensional space as a function of energy and time. The neutron data are derived from the latest nuclear data libraries [2]: ENDF/B-VI 5 (USA), JENDL-3.2 (Japan), JEF-2.2 (Europe), EAF-4.2 (Europe), CENDL-2.1 (China), EFF-2.4 (Europe) and BROND-2 (Russia).

The general architecture of the EA-MC code is shown in Fig. 1. The geometrical description is first automatically translated into FLUKA's combinatorial geometry, and the high-energy particle transport is carried out [3, 4]. Neutrons are transported down to 20 MeV and then handed over to EA-MC which continues the transport.

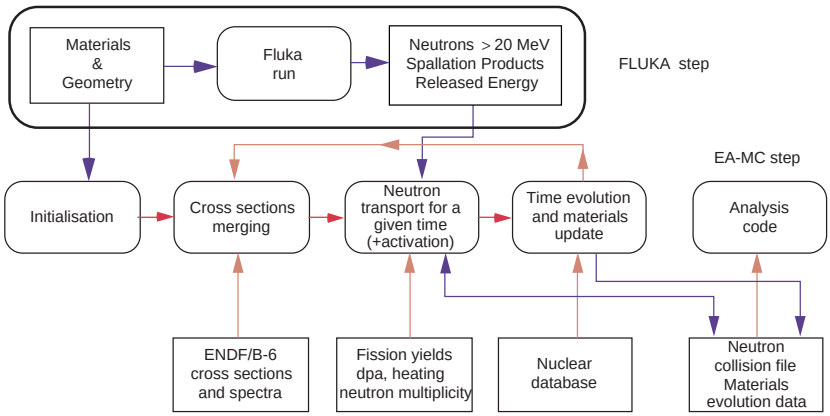

Fig. 1. **General architecture of the EA-MC simulation of neutron transport and element evolution**

The EA-MC code is designed to run both on parallel and scalar computer hardware. Having used standard language elements, the code can be implemented on different systems. A common initialisation section is followed by a parallel phase where every CPU runs an independent simulation with the same initialisation data. A parallel analysis program collects the results and calculates the standard deviation among the different CPUs. This gives an estimate of the statistical fluctuations [5].

The Energy Amplifier Demonstration Facility

The key objective of the Energy Amplifier Demonstration Facility [1], in a first approximation, aims at demonstrating the technical feasibility of a fast neutron operated accelerator-driven system cooled by

molten lead-bismuth eutectic (LBE) and in a second phase that of incinerating TRUs and long-lived fission fragments while producing energy.

Reference configuration

As in the case of the Energy Amplifier's conceptual design [6], the EADF core consists of an annular structure immersed in molten lead-bismuth eutectic which serves as primary coolant and spallation target (Fig. 2). The central annulus contains the spallation target unit which couples the proton accelerator to the sub-critical core. The core is arranged in a honeycomb-like array forming an annulus with four coaxial hexagonal rings of fuel sub-assemblies. The fuel core is itself surrounded by an annular honeycomb-like array of four rings of dummy sub-assemblies, which are essentially empty ducts. The detailed description of the EADF reference configuration can be found in [1].

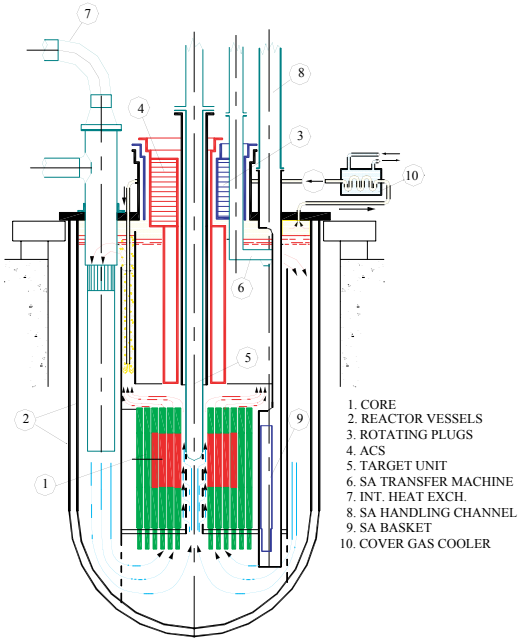

Fig. 2. **Schematic view of the reactor system assembly. [1]**

The coupling of the accelerator system to the sub-critical core is realised via the target unit. The design approach chosen for the EADF [1], has been to keep the spallation products confined where they are generated. The lead-bismuth eutectic spallation target is therefore kept separated from the primary coolant and confined within the structure of the target unit. The target unit structure is located in the central opening of the sub-critical core, which has an equivalent diameter of 630 mm. The beam pipe penetration takes place from the top of the reactor vessel.

Global neutronic parameters at Beginning-Of-Life

The present version of the EA Monte Carlo code package enables a rather complete and detailed model of the EADF reference configuration at the level of individual fuel pins or heat exchanger tubes (presently arranged in square lattices). All the major core components have been taken into consideration.

The main global results for the Beginning-Of-Life performance of the EADF reference configuration are summarised in Tables 1 and 2.

Table 1. **Main Parameters of the EADF reference configuration**

Global Parameters	*Symbol*	*EAP80*	*Units*
Initial fuel mixture	MOX	$(U\text{-}Pu)O_2$	
Initial fuel mass	m_{fuel}	3.793	ton
Initial Pu concentration	m_{Pu} / m_{fuel}	18.1	wt.%
Initial Fissile enrichment	$Pu^{39,41} / U^{38}$	18.6	wt.%
Thermal Power Output	P_{th}	80	MWatt
Proton Beam Energy	E_p	600	MeV
Spallation Neutron Yield	$N_{(n/p)}$	14.51± 0.10	
Neutron multiplication	M	27.80 ± 0.56	
Multiplication Coefficient	k=(M-1) / M	0.9640 ± 0.0007	
Energetic Gain	G	42.73 ± 0.88	
Gain coefficient	G_0	1.54	
Accelerator Current	I_p	3.20 ± 0.07	

Table 2. **Core Power Distributions of the EADF reference configuration**

Av. fuel Specific Power	P_{th} / m_{fuel}	24.5	W / g
Av. fuel power density	P_{th} / V_{fuel}	255	W / cm^3
Av. core power density	P_{th} / V_{core}	55	W / cm^3
Radial peaking factor	P_{max} / P_{ave}	1.25	
Axial peaking factor	P_{max} / P_{ave}	1.18	

Neutronic properties of the different source cases

The effective neutron multiplication factor, k_{eff}, is an intrinsic property of the system. If the flux distribution is not an eigenstate of the operator, the net neutron multiplication factor, k, will be different, but this will not change the value of k_{eff}. We can still formally define a value of k as $k_{src} = 1–1/M_{src}$, but it will depend on the neutron flux as well as on the system. In particular, in the presence of an external source, this value will depend on the position and energy spectrum of the source neutrons. Hereinafter, k_{src} will indicate the value of k calculated from the net multiplication factor M_{src} in the presence of an external source.

By definition, a constant power operation requires ν/k_{eff} neutrons per fission, which means that an external source has to provide a number of neutrons per fission that is:

$$\mu_{eff} = \nu\left(\frac{1}{k_{eff}} - 1\right) = \frac{\nu}{M_{eff} - 1}$$

if they are distributed exactly as the eigenfunction of the stationary problem. In the case of an arbitrary external source, this number becomes

$$\mu_{src} = \nu\left(\frac{1}{k_{src}} - 1\right) = \frac{\nu}{M_{src} - 1} \quad .$$

The ratio

$$\varphi^* = \frac{\mu_{eff}}{\mu_{src}} = \frac{\left(1 - k_{eff}\right)/\left(k_{eff}/\nu\right)}{\left(1 - k_{src}\right)/\left(k_{src}/\nu\right)}$$

is known as the importance of source neutrons. ν^* is an effective number of neutrons per fission and thus contains a correction for non-fission multiplicative processes such as (n,Xn) reactions, which are of great importance for lead-bismuth or lead cooled fast reactors.

The neutronic properties of three different source cases has been examined: a spallation source driven reference configuration (in short: reference or ADS case), a deuteron-deuteron fusion source case (D-D or DD) and a deuteron-triton fusion source case (D-T or DT). As compared with the reference case, the D-D configuration stayed within a range of 260 pcm (1 pcm = $1 \cdot 10^{-5}$) in terms of the neutron multiplication factor (k_{src}), cf. Table 3. The D-T source configuration exhibits a distinctively higher k_{src} than the reference case, the difference in k_{src} being 1500 pcm (0.015). Other central neutronic parameters are shown in Table 4. It should be noted that the required fusion source intensities ("External n/s" in Table 4) are remarkably high. For comparison, it can be mentioned that the source intensity of large-scale inertial confinement fusion experiments reaches a level of ~10^{18} n/s for the higher yielding D-T fusion.

Table 3. **Neutron multiplication factors for the different source configurations**

k_{eff}	k_{src}		
	ADS	Fusion-DD	Fusion-DT
0.9634	0.9640	0.9614	0.9790

Table 4. **Main neutronic parameters for the different source configurations**

	ADS	Fusion-DD	Fusion-DT
φ*	1.0196	0.9478	1.7727
$M=1/(1-k_{src})$	27.8	25.9	47.6
Total n / s	$8.01\ 10^{18}$	$7.98\ 10^{18}$	$8.13\ 10^{18}$
External n / s	$2.88\ 10^{17}$	$3.08\ 10^{17}$	$1.71\ 10^{17}$
fiss / s	$2.50\ 10^{18}$	$2.50\ 10^{18}$	$2.50\ 10^{18}$
ν*	3.09	3.07	3.19
$s_{capt}(U^{238}) / s_{abs}(Pu^{239})$	0.68	0.68	0.68

Since the D-T source configuration case was found to show the most notable differences in comparison with the reference ADS case, the onus will be on comparing the reference ADS and D-T source configuration cases. In Table 5, the neutron balance of the whole EADF device is presented. The fuel core neutron balance is presented in Table 6.

Table 5. **Neutron balance in the whole device.**

Neutron Absorption Inventory	ADS	Fusion-DD	Fusion-DT
Reactor containment	0.32 %	0.32 %	0.32 %
LBE target	1.90 %	1.76 %	3.49 %
Flow guides	0.15 %	0.15 %	0.15 %
Heat exchangers	0.90 %	0.89 %	0.86 %
Purification units	0.03 %	0.03 %	0.03 %
Conv. Enh. units	0.17 %	0.17 %	0.17 %
Neutron shield	2.53 %	2.50 %	2.47 %
Core upper reflector	5.33 %	5.31 %	5.21 %
Core radial reflector	2.05 %	2.03 %	2.00 %
Core lower reflector	6.69 %	6.66 %	6.55 %
Fuel core	72.81 %	73.15 %	71.83 %
Primary coolant	6.69 %	6.66 %	6.55 %
Outs	0.20 %	0.15 %	0.15 %
Total	100 %	100 %	100 %
Main Nuclear Reactions	ADS	Fusion-DD	Fusion-DT
Capture	66.09 %	66.20 %	65.01 %
Fission	31.16 %	31.29 %	30.72 %
n,Xn	2.13 %	1.95 %	3.69 %
Others	0.42 %	0.41 %	0.43 %
Outs	0.20 %	0.15 %	0.15 %
Total	100 %	100 %	100 %

Table 6. **Neutron balance in the fuel core.**

Neutron Absorption	ADS	Fusion-DD	Fusion-DT
Fuel	89.80 %	89.79 %	89.80 %
Cladding	3.77 %	3.78 %	3.77 %
Sub-assembly	1.93 %	1.93 %	1.91 %
Coolant	4.50 %	4.50 %	4.52 %
Main Nuclear Reactions	ADS	Fusion-DD	Fusion-DT
Capture	54.40 %	54.44 %	54.42 %
Fission	42.81 %	42.77 %	42.76 %
n,Xn	2.27 %	2.26 %	2.29 %
Others	0.53 %	0.53 %	0.53 %

From the perspective of the whole device, it is seen that the D-T source produces significantly more reactions in the LBE target than the ADS source does, and leakage is smaller[1]. This increase is linked with a relative decrease of reactions in the fuel core. The composition of reaction types is, in consequence[2],

[1] The slightly higher leakage from the ADS geometry stems from the spatially asymmetrical neutron flux distribution of an ADS source.

[2] The LBE target is inclined for (n,Xn) reactions; capture and other reactions occur relatively infrequently.

altered by an increase of the relative occurrence of (n,Xn) reactions at the expense of capture and fission reactions. Regarding the neutron absorption inventory and the composition of the main reaction types of the core, no particular or distinguishable trends can be reported (cf. Table 6). An explanation for the abundancy of (n,Xn) reactions in the LBE target of the D-T source driven configuration can be sought by studying Fig. 3, which shows the LBE target neutron spectra for the different source configurations. Just around 14 MeV, the spectrum of the D-T driven target shows clearly distinguishable peaks, which arise due to the typical energy distribution of a D-T source. In this energy region, cross sections for both (n,2n) and (n,3n) reactions come close to their maximum, and thus the overall (n,Xn) reaction ratio will increase[3]. Table 7 compares the neutron flux distributions of the cases.

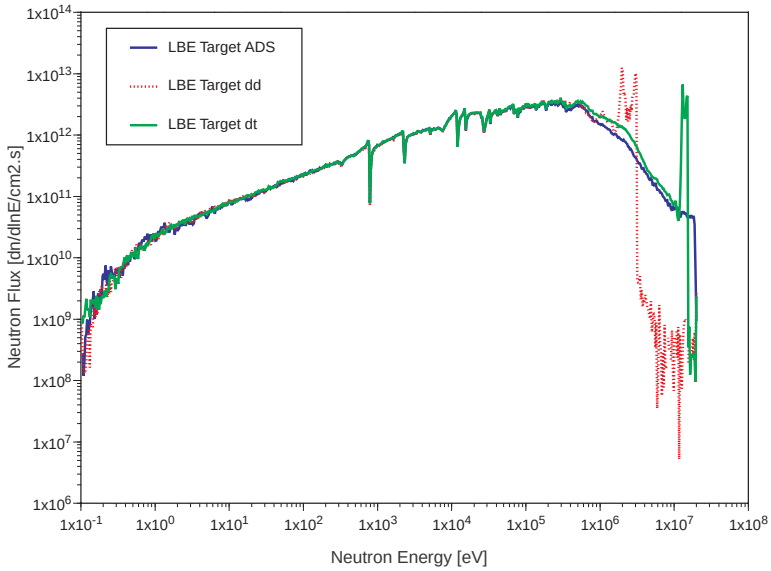

Fig. 3. **LBE target neutron spectra**

Table 7. **Neutron flux distributions throughout the device**

Reactor region	ADS	Fusion-DD	Fusion-DT
Reactor vessel	1.2×10^{11}	1.1×10^{11}	1.2×10^{11}
Safety vessel	3.6×10^{10}	3.5×10^{10}	3.6×10^{10}
LBE target	5.9×10^{14}	6.9×10^{14}	6.6×10^{14}
Target vessel	8.2×10^{13}	8.3×10^{13}	8.3×10^{13}
Heat exchangers	5.8×10^{11}	5.7×10^{11}	5.7×10^{11}
HX secondary coolant	7.2×10^{11}	7.2×10^{11}	7.2×10^{11}
Core neutronic protection	1.5×10^{13}	1.5×10^{13}	1.5×10^{13}
Av. fuel	1.3×10^{14}	1.3×10^{14}	1.3×10^{14}
Av. fuel cladding	3.4×10^{13}	3.4×10^{13}	3.4×10^{13}
Core radial reflector	7.1×10^{13}	7.0×10^{13}	7.0×10^{13}

[3] The neutrons from D-D fusion appear at significantly lower energies, around 2.5 MeV. Thus, they do not produce any significant changes in the overall (n,Xn) reaction occurrence.

As is seen from Table 7 (and Fig. 3), the neutron flux distributions do not differ to any larger extent except for in the LBE target. The characteristical peaks at energies of ~2.5 MeV and ~14 MeV are found for the D-D and D-T fusion sources (respectively). Upon noting that the scale of Fig. 3 is logarithmic and comparing the high energy part of the spectra, it is readily conceived that the integral flux of the fusion cases indeed is higher than that of the reference ADS configuration

The axial and radial neutron flux distributions of all the configurations were examined for possible differences. As can be perceived from Figs. 4, 5 and 6 presenting the results graphically, the only differences are found near the radial centre, where the LBE target is located.

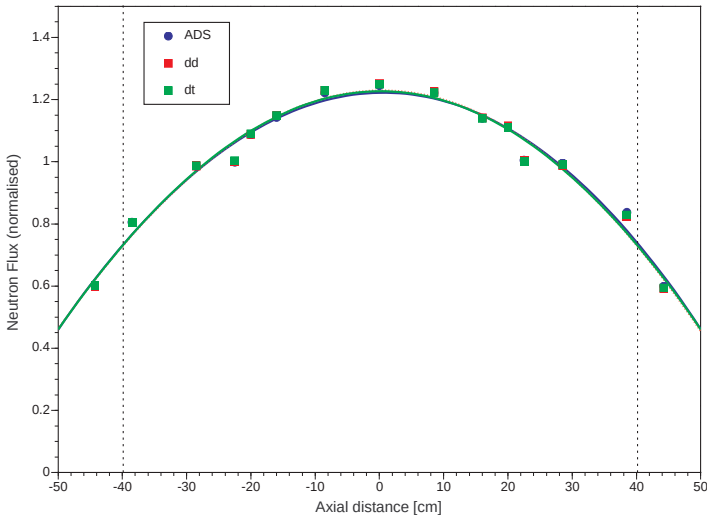

Fig. 4. **Normalised neutron flux distribution over the height of the fuel core**

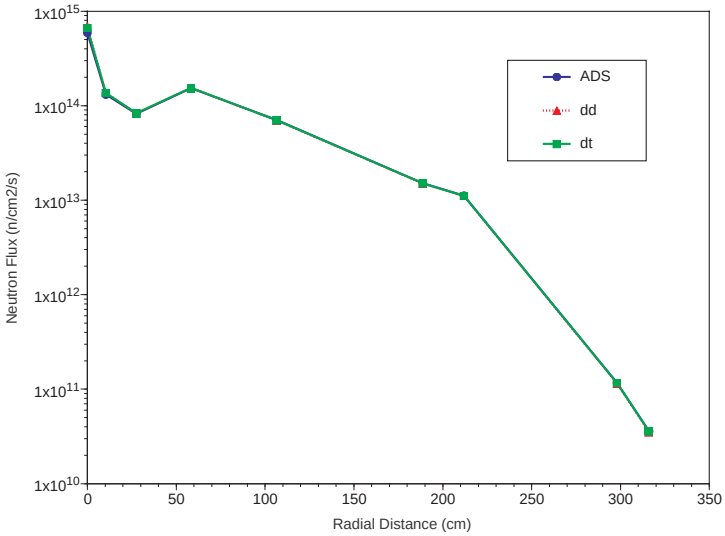

Fig. 5. **Radial distribution of the neutron flux**

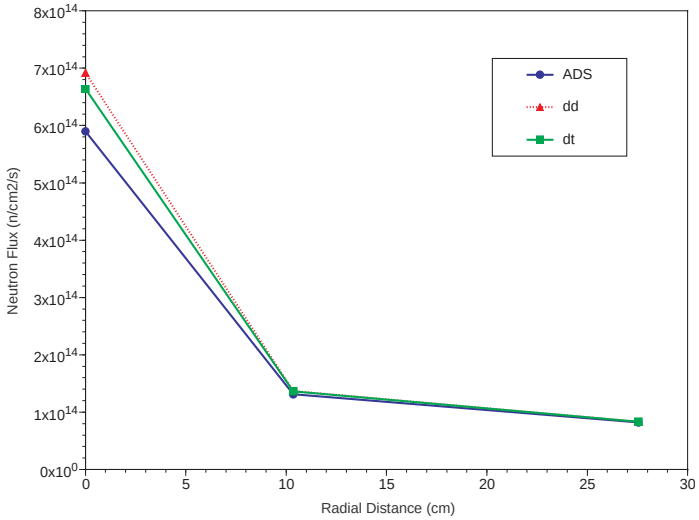

Fig. 6. **Close-up near the LBE target of the radial distribution of the neutron flux**

A direct consequence of an increased high-energy[4] neutron flux load on the LBE target will be a higher displacement rate[5]. The EA-MC code allows for estimation of the damage to structural material from the generated neutron flux spectra, accounting for damage induced by both high-energy particles and low-energy neutrons. Table 8 presents the displacement rate in some of the main structural components. The LBE target serves as an important attenuator of neutron flux and energy, which is clearly recognised from the table: the DPA/year values are similar for the other structural components than the target itself. Both fusion sources produce roughly the double amount of damage than the ADS configuration does, but the damage is effectively absorbed in the target.

Table 8. **Displacement rates**

DPA/year	ADS	Fusion-DD	Fusion-DT
Reactor vessel	8.3×10^{-6}	7.5×10^{-6}	8.1×10^{-6}
Safety vessel	2.5×10^{-6}	2.4×10^{-6}	2.6×10^{-6}
LBE target	1.566	2.988	2.643
Target vessel	0.230	0.235	0.235
Heat exchangers	1.5×10^{-4}	1.5×10^{-4}	1.5×10^{-4}
HX secondary coolant	1.1×10^{-4}	1.1×10^{-4}	1.1×10^{-4}
Core neutronic protection	5.7×10^{-3}	5.6×10^{-3}	5.7×10^{-3}
Av. fuel	0.807	0.808	0.809
Av. fuel cladding	0.152	0.152	0.152
Core radial reflector	0.146	0.145	0.145

[4] Consequences are not so drastic for a higher flux if the spectrum is soft. This is seen in the case of the fission source configuration.

[5] The displacement rate is measured in units of displacement per atom / year (DPA / year).

Table 9 reports the transmutation efficiencies for the nuclides to be destroyed. In the case of ^{238}Pu and ^{241}Pu, the D-T configuration proves to have the most efficient transmuter capabilities, although the difference is slight. This benefit arises due to the harder spectrum of the D-T source (cf. Fig. 3).

Table 9. **Transmutation efficiencies**

Fission / Capture	ADS	Fusion-DD	Fusion-DT
Pu^{238}	1.83	1.85	1.94
Pu^{239}	3.33	3.32	3.33
Pu^{240}	0.66	0.66	0.66
Pu^{241}	6.07	6.05	6.11
Pu^{242}	0.41	0.41	0.41
Np^{237}	0.28	0.52	0.19
Am^{241}	0.13	0.13	0.14

Since the neutron flux distributions were essentially the same throughout the core[6] independent of source configuration, also the transmutation rates remained unaffected by the choice of neutron source. Table 10 presents a comparison between the transmutation rates for the EADF fuelled with (Th-Pu)O_2, the EADF fuelled with (U-Pu)O_2 and a standard PWR fuelled with UO_2.

Table 10. **Transmutation rates (kg/TW$_{th}$h) of plutionium and minor actinides**

Nuclides	EADF (Th-Pu)O_2 ENDF/B-VI	EADF (U-Pu)O_2 ENDF/B-VI	PWR UO_2
^{233}U	+31.0	–	–
Pu	-42.8	-7.39	+11.0
Np	+0.03	+0.25	+0.57
Am	+0.24	+0.17	+0.54
Cm	+0.007	+0.017	+0.044
^{99}Tc prod	+1.08	+1.07	+0.99
^{99}Tc trans	-3.77	-3.77	–

Conclusion

The neutronic properties of four different neutron source configuration of the EADF have been examined by means of 3-D Monte Carlo techniques. The results indicate that the accelerator driven and the fusion-DD source systems would exhibit similar neutronic properties. The fusion-DT source driven configuration differs from the others, giving rise to a neutron multiplication factor ~1500 pcm higher than the others. The effect was seen to be mainly due to the DT-fusion characteristical neutron emission energy spectrum, which produces a significantly larger share of (n,Xn) produced neutrons. Finally, it was established that the choice of source configuration has negligible impact on transmutation efficiencies and transmutation rates.

[6] As earlier was seen, there is a difference between different source configuration for the flux over the LBE target. However, since this region carries no fissile materials, no effect on transmutation rates is seen.

REFERENCES

[1] Ansaldo Nucleare, Energy Amplifier Demonstration Facility Reference Configuration: Summary Report (ANSALDO Nucleare, EA-B0.00-1-200 – Rev. 0, January, 1999).

[2] OECD/NEA, Data Bank (Issy-Les-Moulineaux, Paris, France, 1994).

[3] A. Fassó, A. Ferrari, J. Ranft, P.R. Sala, G.R. Stevenson, J.M. Zazula, Nuclear Instruments and Methods A, 1993, 332, 459, also, CERN report CERN/TIS-RP/93-2/PP (Geneva, 1993).

[4] A. Fassó, et al., Intermediate Energy Nuclear Data: Models and Codes", Proceedings of a Specialists' meeting (Issy-Les-Moulineaux, Paris, France, May 30 – June 1, 1994), p. 271 (OECD, 1994) and references therein.

[5] S. Atzeni, Y. Kadi, C. Rubbia, Statistical Fluctuations in Monte Carlo Simulations of the Energy Amplifier, CERN report CERN/LHC/EET 98-004 (Geneva,, April 20, 1998.

[6] C. Rubbia et al., Conceptual Design of a Fast Neutron Operated High Power Energy Amplifier, CERN report CERN/AT/95-44 (EET) (Geneva, September 29, 1995)